Nano Today 27 (2019) 28–47

Contents lists available at ScienceDirect

Nano Today

journal homepage: www.elsevier.com/locate/nanotoday

Review

Functional T cell activation by smart nanosystems for effective cancer immunotherapy

Weijing Yang[a,c], Zijian Zhou[c], Joseph Lau[c], Shuo Hu[a,b,*], Xiaoyuan Chen[c,**]

[a] Department of PET Center, Xiangya Hospital, Central South University, Changsha, 410008, China
[b] National Clinical Research Center for Geriatric Disorders (XIANGYA), Xiangya Hospital, Central South University, Changsha, 410008, China
[c] Laboratory of Molecular Imaging and Nanomedicine (LOMIN), National Institute of Biomedical Imaging and Bioengineering (NIBIB), National Institutes of Health (NIH), Bethesda, MD 20892, USA

ARTICLE INFO

Article history:
Received 31 December 2018
Received in revised form 18 March 2019
Accepted 21 May 2019
Available online 15 June 2019

Keywords:
Cancer immunotherapy
Smart nanosystems
Artificial antigen presenting cells
Cancer nanovaccine
Tumor microenvironment modulation
Combination therapy

ABSTRACT

Immunotherapy (*e.g.*, checkpoint blockade, adoptive T cell therapy, cancer vaccine) has emerged as one of the most important treatment modalities for cancer in the past two decades. While these approaches are promising, the response rates observed in clinical trials are less than 30% due to tumor heterogeneity and complexity of the tumor microenvironment. Smart nanosystems have the potential to address some of the limitations associated with immunotherapy. Herein, we review applications of nanosystem-mediated immunotherapy for functional T cell activation, including formation of artificial antigen presenting cells, cancer nanovaccination, tumor microenvironment modulation, and combination therapy. Finally, we propose areas of research for the future development of nanosystem-mediated cancer immunotherapy.

Contents

* Corresponding author at: Department of PET Center, Xiangya Hospital, Central South University, Changsha, 410008, China.
** Corresponding author.
E-mail addresses: hushuo_xy@163.com (S. Hu), shawn.chen@nih.gov (X. Chen).

https://doi.org/10.1016/j.nantod.2019.05.004
1748-0132/

Introduction

Immunotherapy, which relies on the activation of a patient's immune system to eliminate cancer, has been attracting more attention because of their clinical efficacy [1]. Conventional immunotherapy can be achieved by functional T cell activation *in vivo* or by reinfusion of activated T cells expanded *in vitro* to kill tumor cells. Checkpoint blockade [2–7], adoptive cell transfer (ACT) [8–12] and cancer vaccine [13–16] are other approaches of immunotherapy that have shown promise in clinical settings. Notably, the 2018 Nobel Prize in Physiology or Medicine was jointly awarded to Drs. James P. Allison and Tasuku Honjo for their pioneering work on immune checkpoint blockade. Although immunotherapy can be very effective, only a small portion of patients respond for the following reasons. First, tumors are heterogeneous and clonal evolution enables them to evade immune surveillance [17]. Different cancers have different sensitivities toward immunotherapy [18], especially for immune checkpoint blockade. ACT therapy is limited by reduced T cell activity over time and potential for autoimmune toxicity [11,19]. Moreover, the tumor microenvironment is host to a myriad of immunosuppressive signals that can negate therapeutic efficacy [20,21]. Therefore, alternative approaches are needed to tackle some of the issues associated with cancer immunotherapy.

Nanosystems have the potential to complement and improve cancer immunotherapy [22–25]. Generally, there are four strategies to induce host immunity using nanosystems. First, artificial antigen presenting cells (aAPCs) [26,27] after specific modifications can imitate natural APCs, especially dendritic cells (DCs), to stimulate T cells residing in lymph nodes. The process requires signaling of the major histocompatibility complex I (MHC I) with T cell receptor (TCR) and co-stimulation signaling of CD80/CD86 expressed on DCs with CD28 on T cells [28–31]. Second, nanoparticles can be used as nanovaccines [32–37] to deliver tumor-associated antigens (TAAs), neoantigens or adjuvants to DCs, which mature and go on to activate T cells. These nanosystems enter the lymph nodes via lymphatic drainage following subcutaneous injections. Nanosystems encapsulated with adjuvant can also accumulate in tumor tissues by passive targeting through the enhanced permeability and retention (EPR) effect [38,39] or by active targeting after ligand functionalization [40–42]. Concomitantly, these nanosystems with encapsulated adjuvants are able to form cancer vaccine *in vivo* after external stimulus combined with excreted TAAs [43–45]. Third, nanosystems loaded with specific inhibitors, siRNA, or phototherapy sensitizers, have the ability to modulate tumor microenvironment through inhibition of immunosuppressive cytokines, depletion of regulatory T cells (T_{regs}) or polarization of tumor-associated macrophages (TAMs) [46–50]. Finally, nanosystems can be modified to mediate [51–53] immunotherapy in combination with chemotherapy, photodynamic therapy (PDT), photothermal therapy (PTT) and/or radiotherapy (RT) [54–57].

Herein, we summarize the use of smart nanosystems for immunotherapy. We will discuss the recent developments of aAPCs, nanosystems induced cancer nanovaccines, tumor microenvironment modulation, and combination therapy for immunotherapy (See Table 1). The prospects of nanosystem-mediated immunotherapy will be discussed with respect to clinical translation. We hope this review can motivate more researchers to engage in cancer immunotherapy using nanotechnology and to identify promising new treatments.

Artificial antigen presenting cells (aAPCs) for functional T cell activation

Antigen processing and presentation by antigen presenting cells (APCs) is important for mounting a functional T cell response. aAPCs are increasingly recognized for their ease of modification, and ability to induce effective T cell immune response. In general, aAPCs need three key factors (Signal I for antigen recognition: MHC-peptide complex or anti-CD3 for antigen specific or non-specific T cell activation; Signal II for co-stimulation: anti-CD28 interacting with CD28 expressed on T cells; Cytokines: interleukin-2 (IL-2), interleukin-12 (IL-12), or interleukin-15 (IL-15) for $CD8^+$ T cell survival or T cell activation) [26,58]. Among the aAPCs, micro-sized aAPCs (maAPCs) and nano-sized aAPCs (naAPCs) are the most studied due to their broad applications in cancer. In the following sections, we will discuss these two forms of aAPCs.

Micro-sized aAPCs

T cell activation through aAPCs is affected by various factors including size, shape and ligand mobility of aAPCs [26,59–61]. In general, maAPCs approximate the size of actual cells and have large surface area for interacting with T cells. However, due to possible embolism *in vivo* especially for those formed by non-degradable materials, maAPCs are generally used for T cell expansion *ex vivo*. The T cells are subsequently reinfused into host for adoptive T cell therapy [62]. For example, Steenblock et al. reported biodegradable maAPCs based on poly (lactic-co-glycolic) acid (PLGA) microparticle coated with anti-CD3 or MHC-peptide complex and anti-CD28 [63]. According to the data, the maAPCs displayed potent T cells expansion *ex vivo* with sustainable IL-2 paracrine release. maAPCs can also be synthesized on mesoporous silica [64,65]. In a recent work, Cheung et al. reported scaffolds mimicking APCs based on mesoporous silica micro-rods (MSRs) for lymphoma therapy (Fig. 1) [65]. The authors claimed that APC mimicking scaffolds (APC-ms) with anti-CD3, anti-CD28 and IL-2 displayed ten-fold higher polyclonal expansion of primary T cells than those by commercial expansion beads (Dynabeads). After replacing anti-CD3 with peptide loaded MHC class I, APC-ms generated more cytotoxic T-cell subpopulations with antigen-specific expansion compared with autologous monocyte-derived dendritic cells (moDCs). APC-ms yielded similar treatment efficacy as Dynabeads in the lymphoma model, despite generating a five-fold higher expansion of CD19 CAR-T cells.

Nano-sized aAPCs

Compared with maAPCs, naAPCs are safer for *in* vivo use and can be easily delivered to lymph node by lymphatic drainage when they are below 100 nm in size [26]. In general, elliptical naAPCs are more effective for T cell activation compared with spherical structures because they form larger immunological synapses (IS) with T cells [59,66]. In addition, naAPCs based on single-walled carbon nanotubes and nanoworms self-assembled from semi-flexible polymers can efficiently stimulate T cells due to increased surface area and TCR cluster formation, respectively [67,68]. Mandal et al. synthe-

Table 1
Examples of different strategies via nanosystems helped for cancer immunotherapy.

Strategies	Subclasses	System	Drug / administration method	Dose	Cancer cell	Ref.
Artificial antigen presenting cells (aAPCs)	Micro-size	(Anti CD3, pMHC, anti CD28)-PLGA-based microparticle (aAPC) (Anti CD3, pMHC, anti CD28 IL-2)-mesoporous silica micro-rods (APC-ms)	Thy1.1^{+}, PMEL CD8^{+} T cell, aAPC/ *i.v.* 19BBz T cells/*i.v.*	1×10^6 1×10^7	B16F10 Raji	[62] [65] [69] [70]
	Nano-size	(MHC-Ig dimer, anti CD28)-Iron-dextran nanoparticle (nano-aAPC) (anti CD3, anti CD28, anti PD-L1)-fucoidan-dextran based iron oxide nanoparticle (IO@FuDex^3)	pmel T cells/ *i.v.* IO@FuDex^3/ *i.v.*	1×10^6 0.175 mg/kg	B16 4T1-Luc CT26	
Cancer nanovaccin-e	Nanovaccine delivery system	(CpG, shRNA, Adpgk)-intertwining DNA-RNA nanocapsules (iDR-NCs) (OVA)-lipo-polysaccharide nanovaccine (OVA-LPS) (Neoantigen)-PEI adsorbed mesoporous silica microrod (PEI-MSR) (OVA, TAA, peptide)-PC7A based nanovaccine	CpG, Adpgk/*s.c.* OVA/ *i.v.* Neoantigen/ *s.c.* OVA, TAA, peptide/ *s.c.*	CpG 100 nmol/kg Adpgk 0.85 mg/kg 25 μg/kg 2.5 mg/kg 25 μg/kg	MC38 — TC-1 B16F10 CT26 B16-OVA B16F10, MC38TC-1	[88] [35] [89] [34]
	Nanosystem induced cancer vaccine	(GM-CSF, CpG, OVA)-Mesoporous silica rods (MSR) (ICG, R837)-PLGA nanoparticle (PLGA-ICG-R837) (FK, ICG, JQ1)-hydrogel (CpG, cancer cell membrane)-PLGA nanoparticle	OVA/ *s.c.* R837, ICG/ *i.v.* ICG, JQ1/ *s.c.* CpG/ *s.c.*	2.5 mg/kg R837 6 mg/kg ICG 8 mg/kg ICG 2.5 mg/kg JQ1 3.4 mg/kg CpG 8.75 nmol/kg	EG.7 OVA 4T1 CT26 4T1 EMT6 B16F10	[96] [43] [44] [97]
Tumor microenviro-nment (TME) modulation	Cytokines	liposome-protamine-DNA (LPD) nanoparticles (SB505124, IL-2)- liposomal nanogel based on cyclodextrins	Plasmid/ *i.v.* SB505124, IL-2/*i.t.*	2.5 mg/kg SB505124 10 mg/kg IL-2 2.5 μg/kg	KPC98027 RFP/Luc B16	[46] [47]
	Regular T cells (Tregs)	(cyclophosphamide)-platelets presenting PD-1 (IR-780, imatinib)-GITR-PLGA nanoparticles	Cyclophospham-ide/ *i.v.* IR-780, imatinib/*i.v.*	20 mg/kg IR-780 8 mg/kg Imatinib	B16F10 B16/BL6, MC38	[48] [105]
	Tumor-associated macrophage-s (TAMs)	(siCD115)-M2-like TAM dual targeting lipid nanoparticles (M2NP-siCD115) (ICG, TiO_2, NH_4HCO_3)-mannose based PLGA nanoparticles	siCD115/*i.v.* ICG, TiO_2/*i.v.*	5 mg/kg ICG 4 mg/kg TiO_2 0.22 mg/kg	B16 4 T1 B16	[109] [49]

Combinatio-n therapy	Chemotherapy	(oxaliplatin, indoximod)- mesoporous silica nanoparticles (Paclitaxel, IL-2)- two opposite charged chitosan derivatives /2-Hydroxypropyl-β-cyclodextrin (HP-β-CD) based nanogel (Mitoxantrone, celastrol)-aminoethylanisamide-ligand-polymer-nanoparticle (Gemcitabine, anti PD-L1)-Scaffold based on PVA	Oxaliplatin Indoximod/ *i.v.* Paclitaxel IL-2/ *i.v.* Mitoxantrone, celastrol/ *i.v.* Gemcitabine, anti PD-L1/*p.t.*	Oxaliplatin 1.25 mg/kg *(i.t.)* 5 mg/kg (*i.v.*) Indoximod 12.5 mg/kg *(i.t.)* 50 mg/kg (*i.v.*) Paclitaxel 10 mg/kg IL-2 2.5 μg/kg Mitoxantrone 0.8 mg/kg celastrol 0.16 mg/kg Gemcitabine 5 mg/kg anti PD-L1 2.5 mg/kg	PDAC B16F10 BPD6 B16F10	[114] [55] [116] [115]
	Photodynamic therapy (PDT)	(siPD-L1, MTPP)-micelleplexes based on PEG-CDM-PDEA, PEI-PDEA (oxaliplatin, pyropheophorbide)-lipid core-shell nanoparticels (Protoporphyrin, 1-methyltryptophan)-prodrug nanoparticle formed by peptide (siPD-L1, pheophorbide A)-micelleplexes based on PDPA-PPa, OEI-C14	siPD-L1, MTPP/ *i.v.* .Oxaliplatin, pyropheophorbi-de/ *i.p* Protoporphyrin, 1-methyltryptop-han/ *i.v.* siPD-L1 pheophorbide A/ *i.v.*	siPD-L1 0.52 mg/kg MTPP 2 mg/kg oxaliplatin 2 mg/kg pyropheophorbide 16 nmol/kg Protoporphyrin 3 mg/kg 1-methyltryptophan 1 mg/kg siPD-L1 0.31 mg/kg pheophorbide A conjugated micelle 25 mg/kg	B16F10 MC38 HT29 CT26 B16F10	[121] [122] [123] [125]
	Photothermal therapy (PTT)	(DOX)-PDA coated spiky gold nanoparticles (NLG919-IR780)-micelles based on mPEG-PCL (ICG, DOX)-CPCI-nanoparticle	DOX/*i.t.* NLG919, IR780/ *i.v.* ICG, DOX/ *i.v.*	1.36 mg/kg NLG919 6 mg/kg IR780 2 mg/kg ICG 7 mg/kg DOX 2.5 mg/kg	CT26 TC-1 4T1 OSC-3	[128] [126] [129]
	Radiotherapy (RT)	Antigen-capturing nanoparticles based on PLGA (AC-NPs) (^{131}I-catalase, CpG)-containing sodium alginate (ALG) for *in situ* hydrogel (IDOi,)-nanoscale metal-organic framework	AC-NPs/ ^{131}I, catalase, CpG, ALG/ *i.t.* IDOi, DBP-Hf/ *i.t*	100 mg/kg ^{131}I 50 μ Ci /mouse Catalase 0.625 mg/kg CpG 0.5 mg/kg ALG 6.25 mg/kg IDOi 0.56 mg/kg DBP-Hf 5.5 mg/kg	B16F10 4T1 4T1 CT26 SQ20B, U87, PC-3, CT26	[130] [132] [133]

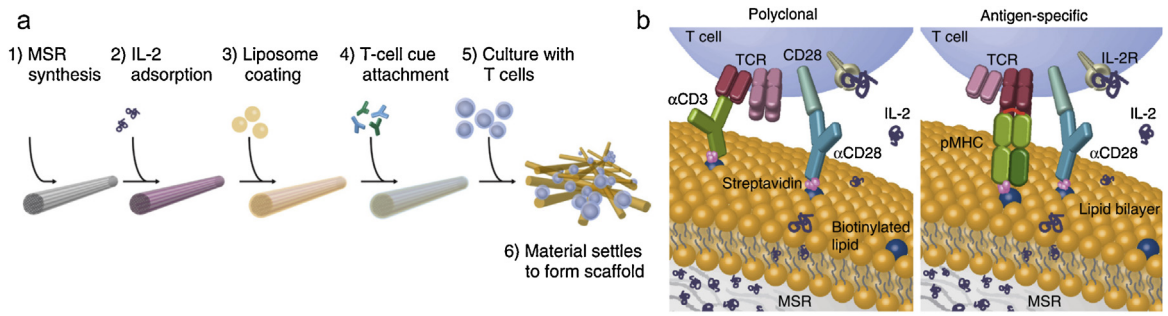

Fig. 1. APC-mimetic scaffolds (APC-ms). (a) Process for preparing APC-ms from MSRs. (b) For polyclonal T-cell expansion, antibodies against CD3 (αCD3) and CD28 (αCD28) are attached (left). For antigen-specific T-cell expansion, peptide-loaded MHC (pMHC) and αCD28 are attached (right). In both cases, IL-2 is released over time, resulting in paracrine delivery to local T cells. Adapted from ref. [65] with permission of Nature Publishing Group, Copyright 2018.

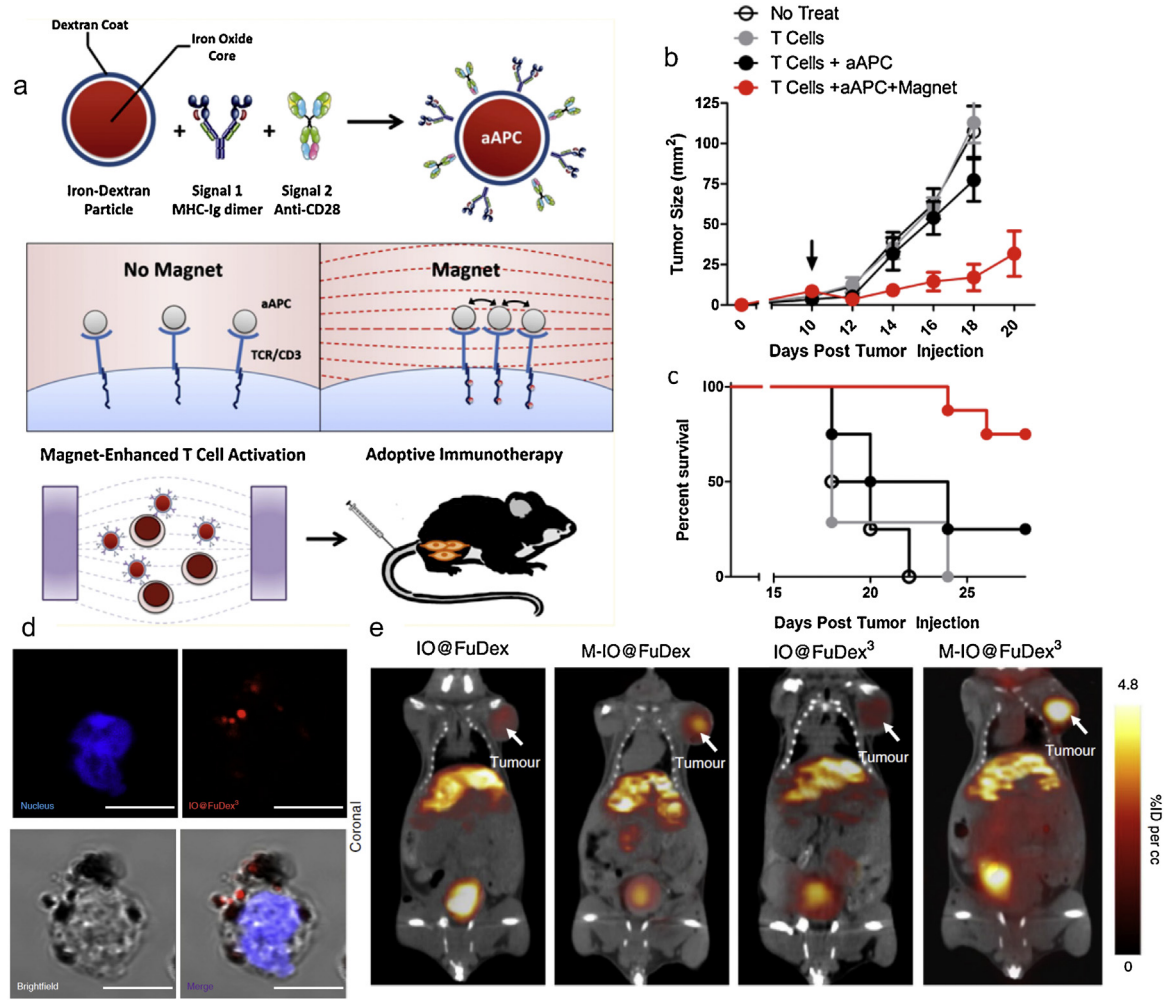

Fig. 2. (a) Schematic of nano-aAPC synthesis by coupling MHC-Ig dimers and co-stimulatory anti-CD28 to iron dextran nanoparticles. (b, c) Treatment with magnet-enhanced nano-aAPC-activated T cells attenuated tumor growth compared to no magnet and control groups. Adapted from ref. [69] with permission of American Chemical Society, Copyright 2014. (d) Fluorescent microscopy images of $CD8^+$ T cells showed cell association with QD-labelled IO@FuDex3 after 30 min incubation. (scale bar, 5 μm). (e) Whole-body, single-photon emission computed tomography images of ^{125}I-labelled IO@FuDex^3 at 24 h after treatment with or without magnetic navigation. Adapted from ref. [70] with permission of Nature Publishing Group, Copyright 2018.

sized vermiform naAPCs based on filamentous and semi-flexible polymers with anti-CD3 decoration [68]. Their results revealed that the naAPCs could not only activate T cells at lower concentration compared with free antibody and rigid naAPCs (PLGA particles), but also induced a more potent T cell response. In addition to size and shape, TCR pre-clustering on T cells is another factor that affects T cell response. Perica et al. used a magnetic field to induce T cell clustering via naAPCs based on iron nanoparticles for immunotherapy (Fig. 2a) [69]. They showed that the naAPCs displayed 2-fold higher binding to clustered TCRs on activated T cells compared with naïve T cells. According to their results, the magnetic field (0.2 T, 30 min) could cause paramagnetic nAPCs aggregation, doubling of TCR cluster size and expansion *in vitro*. The pre-activated T cells showed significant inhibition of B16 melanoma xenografts and prolonged survival time after adoptive transfer therapy (Fig. 2b & c). naAPCs with specific antibody modifications on the particle sur-

face can also activate T cells in bloodstream. Chiang et al. reported a therapeutic fucoidan-dextran-based magnetic iron oxide nanoparticle (IO@FuDex^3) coupled with a checkpoint inhibitor (anti-PD-L1) and T cell activators (anti-CD3 & anti-CD28) [70]. They found that the functionalized IO@FuDex^3 could facilitate checkpoint blockade and T cell proliferation simultaneously. The results shown in Fig. 2 d revealed that IO@FuDex^3 could be adsorbed onto CD8$^+$ T cell membrane. Based on single-photon emission computed tomography imaging, ^{125}I-labelled IO@FuDex^3 had highest tumor accumulation compared to other formulas (Fig. 2e).

Nanosystems mediated vaccination for functional T cell activation

Nanovaccines can efficiently deliver tumor-specific antigen (neoantigen) and adjuvant to APCs to indirectly activate T cells. Moreover, nanosystems encapsulating adjuvants can accumulate in tumor tissues by the EPR effect. When an external stimulus is applied, the nanoformulation causes tumor necrosis and apoptosis, which leads to the secretion of neoantigens and tumor associated antigens (TAAs) forming cancer vaccines *in situ*.

Nanovaccine delivery system

Subunit vaccines including TAAs, neoantigens, adjuvants possess immense potential for cancer immunotherapy. However, their clinical efficacy is limited by inferior delivery to lymph nodes [33]. Nanosystems equipped with proper vehicles are capable of co-delivering antigens and adjuvants to lymphoid tissues and APCs [36,71]. In addition, the nanosystems themselves can also serve as adjuvants to enhance therapeutic efficacy [32,34,72]. We will discuss each of these aspects in the following sections.

Nanovaccine loaded with adjuvants

Constituents of nanovaccines are generally antigens (*e.g.* neoantigens, and TAAs) and adjuvants, including inorganic compounds (*e.g.* aluminum hydroxide, and calcium phosphate hydroxide), cytosine-guanine oligodeoxynucleotides (CpG), polyinosinic polycytidylic acid (poly(I:C)), and imiquimod (R837) [36,73–82]. Following nanosystem-mediated delivery, antigens could be processed into small fragments and presented via MHC class I and MHC class II complexes on the cell surface, which can be recognized by CD8$^+$ and CD4$^+$ T cells, respectively. Adjuvant plays a vital role in increasing APC recognition, antigen translocation to cell surface, and secretion of inflammatory factors [83–85]. Aluminum-containing adjuvants have been approved by the United States Food and Drug Administration (FDA) [86] for human use due to favorable safety profiles. However, traditional aluminum can form microparticles (1–20 μm) when dispersed in solution, which limits APCs uptake and decreases vaccine efficacy [87]. Li et al. reported aluminum hydroxide nanoparticles as adjuvant to avoid aggregation into microparticles; the formula showed high potency after antigen adsorption [74]. In addition, toll-like receptor agonists like CpG and R837, are widely used as adjuvants. In our previous work, nanocapsules loaded with CpG, short hairpin RNA targeting STAT3 (immunosuppressive marker) and neoantigen formed a synergistic nanovaccine that induced potent and continuous adaptive immune response (Fig. 3a-c) [88]. The nanovaccine based on nanocapsules resulted in an increase of CD8$^+$ T cells, and memory T cells compared to free CpG, and enhanced inhibition of a syngeneic colon cancer model. Qiu et al. used lipo-polysaccharide (LPS) mixed with antigen ovalbumin (OVA) or NY-ESO-1 for self-assembly of a nanovaccine. After coating with polyphenol and pH (low) insertion peptide (pHLIP), the nanovaccine showed fast escape from endosome, promoted cytoplasmic localization, enhanced antigen presentation by DCs and activated CD8$^+$ T cells (Fig. 3d) [35].

Nanovaccine using nanomaterials as adjuvants

In addition to loading adjuvants, some nanocarriers as well as microcarriers have intrinsic adjuvant properties. They can induce IL-β production, activate stimulator of interferon genes (STING) signaling pathway or serve as antigen depots [34,89–92]. Li et al. reported a personalized vaccine based on mesoporous silica microrod (MSR) vaccine for polyethyleneimine (PEI) adsorption to enhance antigen immunogenicity (Fig. 4a) [89]. The authors indicated that PEI served as an adjuvant (Fig. 4b & c) causing endosomal disruption, phagosomal content release and IL-1β production. They claimed that the MSR-PEI vaccine significantly enhanced DCs activation and T cells response compared with MSR vaccine and bolus vaccine. According to the author, the MSR-PEI vaccine revealed remarkable tumor inhibition in TC-1, B16F10 and CT26 tumor models. Xia et al. developed micro-size Pickering emulsions as adjuvant by forming antigen OVA depot using squalene as dispersion phase, and PLGA nanoparticles as colloidal stabilizers (Fig. 4d) [91]. The Pickering emulsion enabled antigens to freely diffuse within the droplet leading to multivalent interaction with APC for phagocytosis and activation. Fig. 4e & f illustrated that the Pickering emulsion adjuvant system (PPAS) significantly increased expression of CD86 and SIINFEKL-MHC-I on DC surface after combination with antigen. The authors showed that it could induce CD3$^+$ CD4$^+$ T cell activation in draining lymph node, and increase interferon-γ (IFN-γ) secreting CD8$^+$ T cells and OVA-specific CTLs. Collectively, these processes led to impressive EG7/OVA tumor inhibition. Compared with microcarriers, nanocarriers possess distinct advantages in lymphatic drainage and endocytosis because of smaller size. A STING-dependent nanovaccine based on PC7A micelle developed by Luo et al. elicited a very strong cytotoxic T cell response (Fig. 4g) [34]. The author showed that PC7A nanoparticles serving as adjuvant had strong luminal buffer ability in the endosome, inducing cytosolic delivery of biologics and retaining STING by direct binding. After loading ovalbumin (OVA), OVA-PC7A nanoparticle displayed the highest expression of OVA-H2K^b compared with other three groups (Fig. 4h). In combination with anti-PD-1, the nanovaccine revealed robust tumor growth inhibition in three different tumor models, achieving 100% survival after 60 days in the TC-1 tumor model. Ding et al. prepared large-pore mesoporous-silica-coated upconversion nanoparticles (UCMSs) as immunoadjuvant encapsulation with photosensitizers merocyanine 540 (MC540) and OVA (UCMSs-MC540-OVA) or tumor cell fragment (TF) (UCMSs-MC540-TF)(Fig. 4i) [32]. Their results showed that under laser irradiation UCMSs-MC540-OVA had immune stimulation for Th1, Th2 immune response and high CD4$^+$, CD8$^+$, effector T cells activation. In addition, they found that UCMSs-MC540-TF displayed stronger antitumor efficacy and prolonged survival rate compared with photodynamic therapy or immunotherapy alone in CT26 tumor-bearing mice. Please see the abbreviation in the main text in Table 2.

Nanosystems induced cancer vaccine

Cancer vaccine is a powerful means of activating a host's immune response. Cancer vaccines can be classified into categories based on its composition: whole tumor cell vaccine, DC-based vaccine, peptide/protein-based cancer vaccine, and gene (DNA/RNA) encoded vaccine [93]. Sipuleucel-T is the first therapeutic cancer vaccine approved by the U.S. FDA in 2010 for prostate cancer treatment [16]. However, the immune response generated by conventional cancer vaccine is limited by tumor heterogeneity as well as the presence of immunosuppressive factors. Nanosystems can serve as effective vectors to transport adjuvants, immune negative

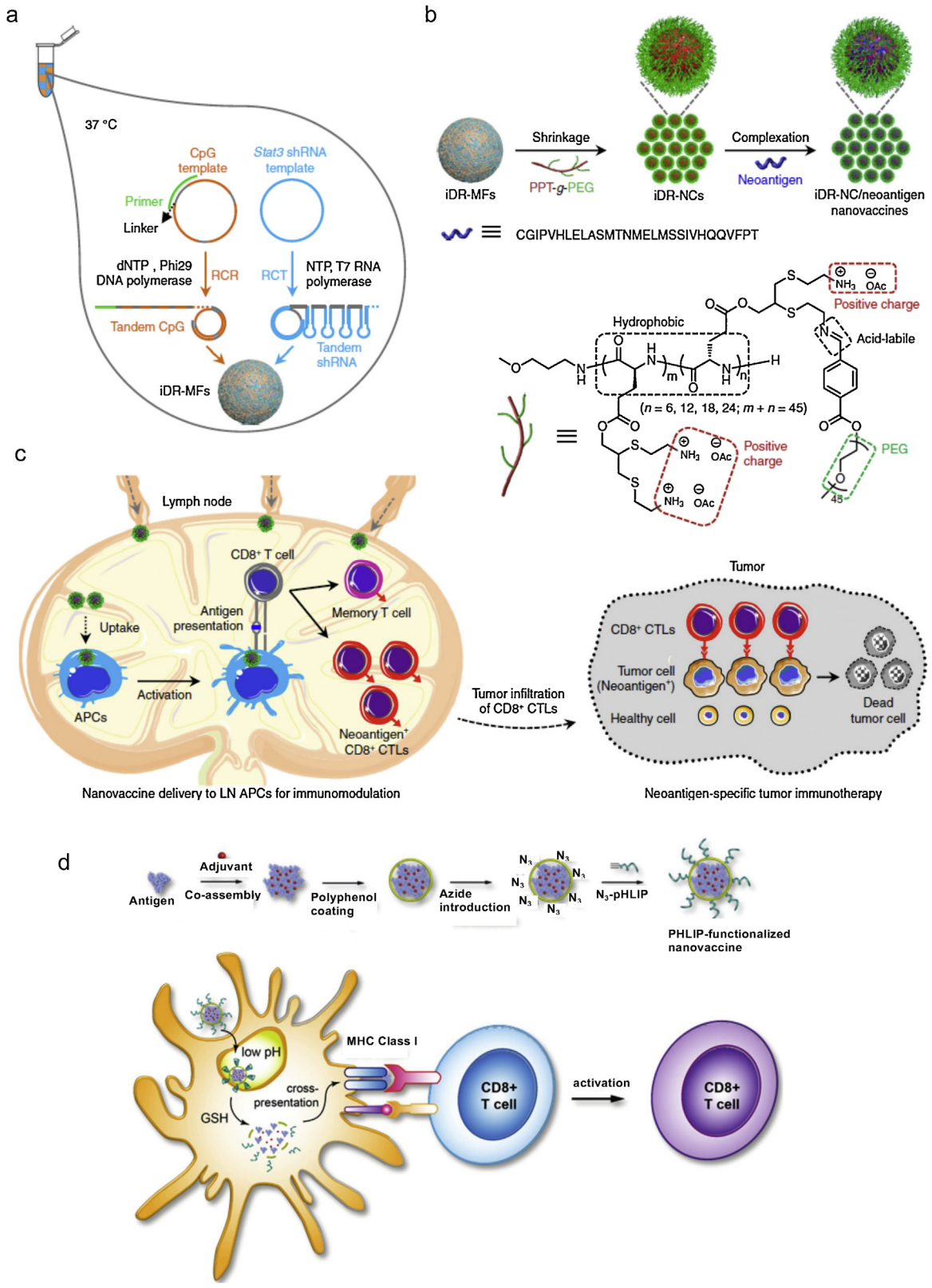

Fig. 3. Schematics of iDR-NC/neoantigen (intertwining DNA-RNA nanocapsule neoantigen) nanovaccines for synergistic tumor immunotherapy. (a) Concurrent rolling circle replication (RCR) and rolling circle transcription (RCT) in the same solution generated tandem CpG and Stat3 shRNA, which were self-assembled into intertwining DNA-RNA MFs (micro-flowers). (b) The above MFs were shrunk by PPT-*g*-PEG to form iDR-NCs, which was further loaded with tumor-specific neoantigen. (c) In immunocompetent mice, iDR-NCs/neoantigen complexes were delivered into APCs in draining LNs, elicited potent and durable neoantigen-specific T cell response, and inhibited tumor progression. Adapted from ref. [88] with permission of Nature Publishing Group, Copyright 2017. (d) Synthesis of the pHLIP-functionalized nanovaccine and working principle of the pHLIP-functionalized nanovaccine for enhanced cytotoxic $CD8^+$ T cell activation. Adapted from ref. [35] with permission of WILEY-VCH Verlag GmbH & Co. KGaA, Weinheim, Copyright 2018.

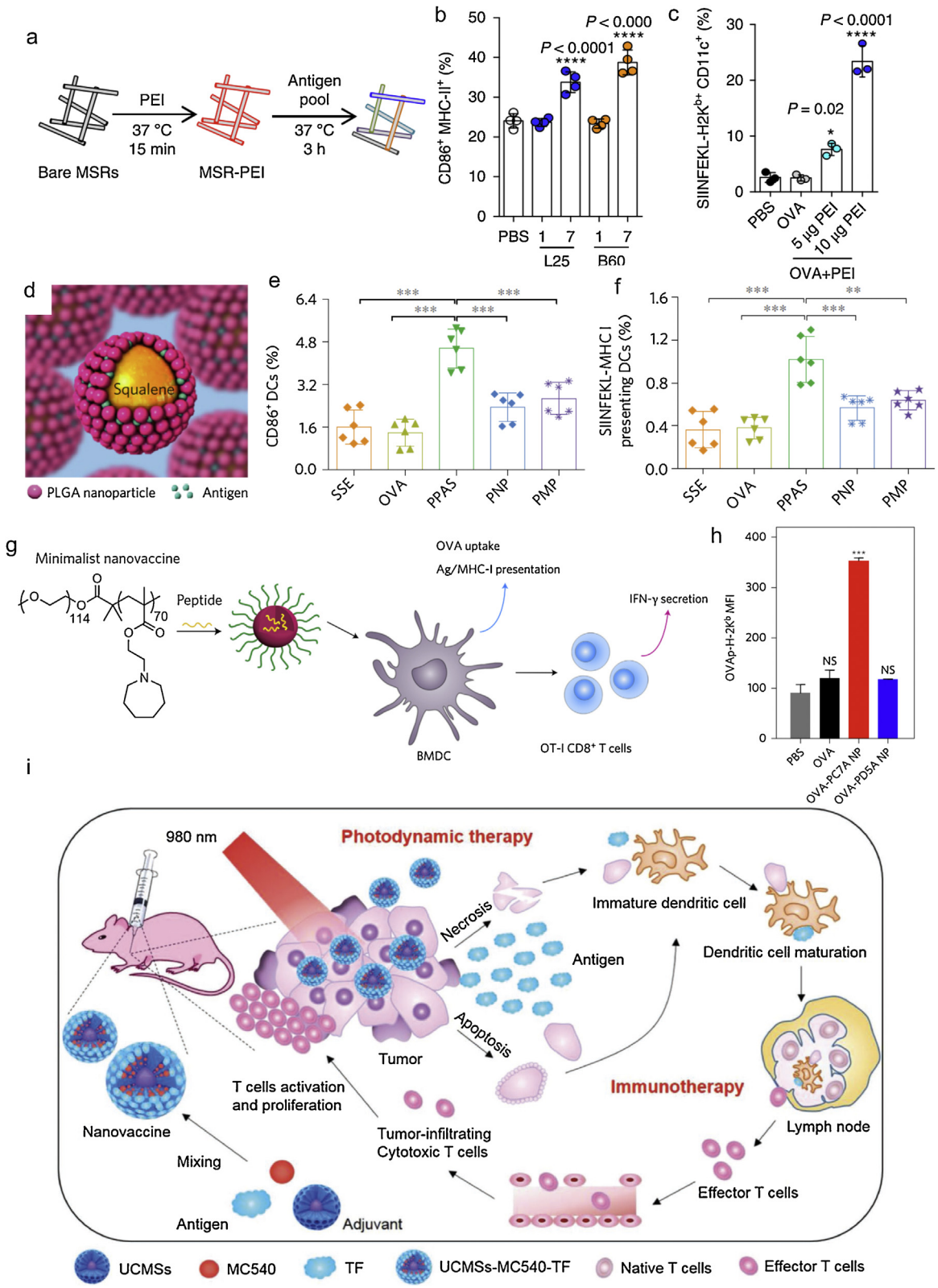

Fig. 4. (a) Schematic representations of PEI and subsequent antigen adsorption onto bare MSRs. (b) Flow cytometry analysis of CD86 and MHC-II expression on murine bone-marrow-derived dendritic cells (BMDCs) after 24 h of stimulation with 1 μg or 7 μg of soluble PEI or PBS. L25 represents 25 K linear PEI and B60 means 60 K branched PEI. (c) Flow cytometry analysis of SIINFEKL-presenting murine BMDCs after stimulation with PBS, OVA, and OVA with 5 μg or 10 μg of soluble B60 K PEI. Adapted from ref. [89] with permission of Nature Publishing Group, Copyright 2018. (d) Schematic representation of PPAS. (e, f) Flow cytometry analysis on the expression of $CD86^+$ (e) and SIINFEKL-MHC I^+ (f) of recruited DCs 24 h post administration. Adapted from ref. [91] with permission of Nature Publishing Group, Copyright 2018. (g) Schematic of the minimalist design of the PC7A nanovaccine. (h) Levels of antigen presentation on H-$2K^b$ in BMDCs induced by PC7A or PD5A NPs. Adapted from ref. [34] with permission of Nature Publishing Group, Copyright 2017. (i) Schematic illustration of fabrication and mechanism of UCMSs-MC540-TF nanovaccines for photodynamic immunotherapy. Adapted from ref. [32] with permission of WILEY-VCH Verlag GmbH & Co. KGaA, Weinheim, Copyright 2018.

Table 2
A list of abbreviation in the main text.

Abbreviation	Full name	Abbreviation	Full name
aAPCs	artificial antigen presenting cells	PTA	photothermal ablation
APCs	antigen presenting cells	PVAX	personalized cancer vaccine
TME	Tumor microenvironment	PD-L1	programmed death-ligand 1
ACT	adoptive cell transfer	IL-6	interleukin-6
DCs	dendritic cells	IL-12p40	interleukin-12 p40
MHC I	major histocompatibility complex I	TNF-α	tumor necrosis factor-α
TCR	T cell receptor	GM-CSF	granulocyte-macrophage colony-stimulating factor
TAAs	tumor-associated antigens	CXCL10	C-X-C motif chemokine 10
EPR	enhanced permeability and retention	FasL	Fas ligand
Tregs	regulatory T cells	VEGF	vascular endothelial growth factor
TAMs	tumor-associated macrophages	CXCL12	C-X-C motif chemokine 12
PDT	photodynamic therapy	CXCL8	C-X-C motif chemokine 8
PTT	photothermal therapy	TGF-β	transforming Growth Factor Beta
RT	radiotherapy	LPD	liposome-protamine-DNA
IL-2	interleukin-2	TAMs1	M1 macrophages
IL-12	interleukin-12	TAMs2	M2 macrophages
IL-15	interleukin-15	anti-CSF-1R	anti-colony stimulating factor I receptor
maAPCs	micro-sized aAPCs	Tfr	transferrin receptor
naAPCs	nano-sized aAPCs	ROS	reactive oxygen species
PLGA	poly (lactic-co-glycolic) acid	TiO_2	titanium dioxide
MSRs	mesoporous silica micro-rods	NH_4HCO_3 or N	ammonium bicarbonate
APC-ms	APC mimicking scaffolds	ICD	immunogenic cell death
moDCs	monocyte-derived dendritic cells	IDO	indoleamine-pyrrole 2,3-dioxygenase
IS	immunological synapse	PDAC	pancreatic ductal adenocarcinoma
CpG	cytosine-guanine oligodeoxynucleotides	IND	indoximod
poly(I:C)	polyinosinic polycytidylic acid	MIT	mitoxantrone
R837	imiquimod	CEL	celastrol
FDA	Food and Drug Administration	TGF-β	transforming Growth Factor Beta
LPS	lipo-polysaccharide	GEM	gemcitabine
OVA	ovalbumin	MDSCs	myeloid-derived suppressor cell
pHLIP	polyphenol and pH (low) insertion peptide	PpIX-1 MT	peptide C16-K(PpIX)-PEG8-KDEVD-1 MT
STING	stimulator of interferon genes	PpIX	photosensitizer protoporphyrin
MSR	mesoporous silica microrod	1 MT	1-methyltryptophan
PEI	polyethyleneimine	(PPa)	photosensitizer pheophorbide A
PPAS	Pickering emulsion adjuvant system	HSP	heat shock protein
IFN-γ	interferon-γ	PCI	PEG5K-CA4-ICGD4
UCMSs	mesoporous-silica-coated upconversion nanoparticles	PCLC	EG5K-Cys4-L8-CA8
MC540	merocyanine 540	Mal	maleimide
TF	tumor cell fragment	AC-NPs	antigen-capture nanoparticles
ICG	indocyanine green	nMOF	nanoscale metal-organic framework
CTLA-4	Cytotoxic T-lymphocyte antigen-4	BiTEG	bispecific T-cell engaging antibodies
HAuNS	hollow gold nanoshells	PET	positron emission tomography
APP	anti PD-1 peptide	SPECT	single-photon emission computerized tomography
AA@PN	AUNP12 in PLGA nanoparticle	MRI	magnetic resonance imaging

modulator inhibitors, or photosensitizers to overcome the above issues [43,44,94,95]. In the following section, we will concentrate on cancer vaccination *in vivo* and *in vitro* mediated by nanosystems.

Cancer vaccination in vivo

In situ cancer vaccination generally depends on DCs recruitment *in vivo*. The DCs capture antigens and adjuvants, maturate, migrate to lymph node, and induce T cell activation. For example, Kim et al. reported that mesoporous silica rods (MSRs) can spontaneously assemble to form macroporous structure *in vivo*. They found that the macroporous structure recruited DCs after an inflammation response due to the release of adjuvant and antigen from the scaffold [96]. Based on their results, the MSR-mediated vaccine indicated strong helper T cell response and increased $CD8^+$ T cells level compared with bolus control. Chen et al. used immune-adjuvant nanoparticles combined with immune checkpoint inhibitor after tumor photothermal ablation to form an *in situ* vaccine (Fig. 5a) [43]. The authors co-encapsulated the photothermal agent indocyanine green (ICG) and R837 in a PLGA self-assembly to form PLGA-ICG-R837 nanoparticles. They reasoned that photothermal ablation of primary tumors can generate TAAs, which can combine with the adjuvant-nanoparticle to produce a cancer vaccine. After combination with anti-cytotoxic T-lymphocyte antigen-4 (CTLA-4), PLGA-ICG-R837 was able to eliminate primary tumors, inhibition secondary tumor growth, and prevented tumor recurrence in 4T1 and CT26 tumor models. In another report, Luo et al. exploited the co-encapsulation of a photothermal agent, hollow gold nanoshells (HAuNS) and an anti-PD-1 peptide AUNP12 (APP) in PLGA nanoparticle (AA@PN) for primary tumor inhibition by photothermal ablation (PTA) and checkpoint inhibition (Fig. 5b) [94]. When combined with CpG adjuvant, the nanoparticle functioned like a vaccine and elicited antitumor immunity. According to their results, AA@PN under laser irradiation plus CpG revealed the highest co-expression of $CD80^+$ and $CD86^+$ on DC surface for *in vitro* co-culture and transwell systems, compared with CpG or AA@PN alone. They claimed that PTA combination with PD-1/PD-L1 checkpoint inhibition for sustainable APP release could eliminate growth of primary tumor (4T1) and metastatic tumors (4T1 & Luci-CT26).

Cancer vaccination in vitro

Another type of cancer vaccination is to use isolated cancer cells to encapsulate adjuvant or directly use cancer cell membrane coatings to form cancer vaccines *in vitro*. These vaccines were

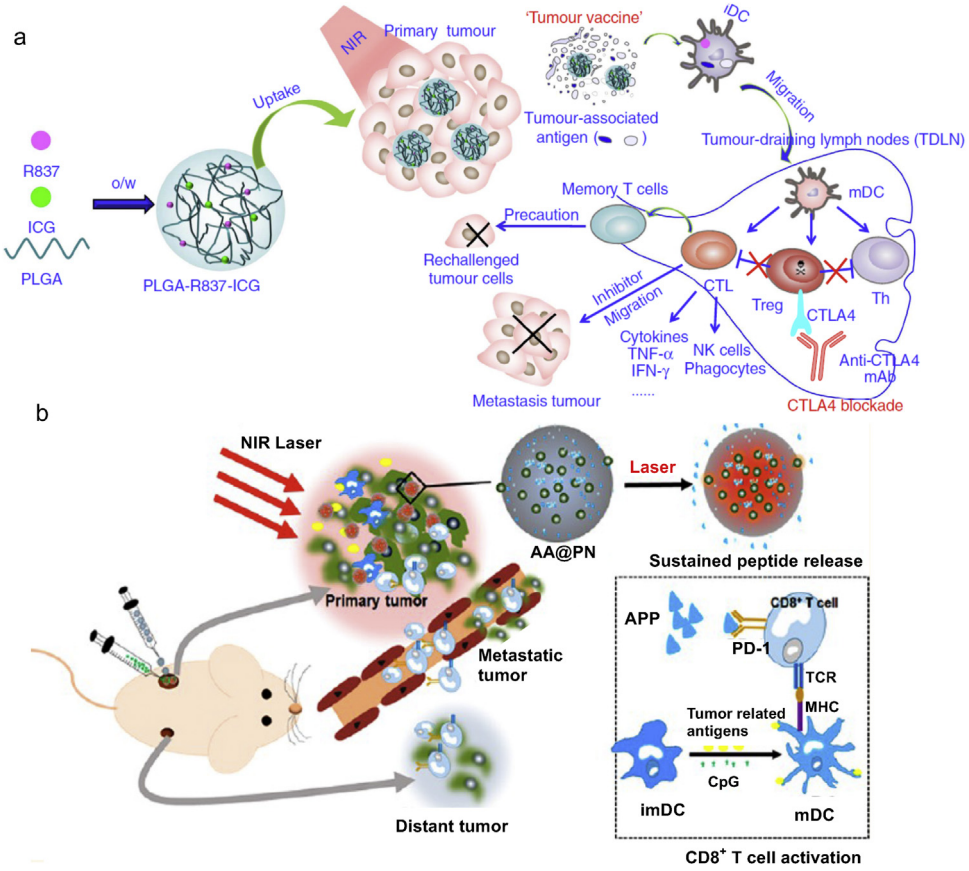

Fig. 5. (a) The mechanism of anti-tumor immune responses induced by PLGA-ICG-R837-based PTT in combination with checkpoint-blockade. Adapted from ref. [43] with permission of Nature Publishing Group, Copyright 2016. (b) Schematic illustration of laser immunotherapy combined with perdurable PD-1 blockade immunotherapy. Adapted from ref [94]. with American Chemical Society, Copyright 2018.

reportedly able to inhibit autologous tumor growth and recurrence after injection [44,95,97]. For example, Wang et al. reported a personalized cancer vaccine that can prevent tumor relapse at surgical site and distant metastasis (Fig. 6a&b) [44]. The authors developed a personalized cancer vaccine (PVAX) based on *co*-loading of JQ1 (programmed death-ligand 1 (PD-L1) inhibitor) and ICG in whole 4T1 cancer cells with FK (penetration peptide) hydrogel matrix (called FK@IQ-4T1). Recurrent tumors treated with FK@IQ-4T1 and laser irradiation at surgical site showed complete regression in 59 days. They also demonstrated distant tumor inhibition and tumor-specific immune response with autologous and allogeneic cancer cells. Kroll et al. constructed cancer cell membrane displaying multiple autologous antigens encapsulated with CpG (CpG-CCNPs) as immune adjuvant to elicit host immunity (Fig. 6c) [97]. The vaccine induced DC maturation with high expression of CD80 and CD86, cytokines secretion (interleukin-6 (IL-6), interleukin-12 p40 (IL-12p40)) and $CD8^+$ T cell activation. In combination with anti-CTLA-4 and anti-PD-1 therapy, CpG-CCNPs demonstrated efficient tumor growth inhibition in B16F10 tumor model, compared with cancer vaccine alone or antibodies alone. The above examples illustrate the synergistic potential of nanoparticulate cancer vaccines with other immunotherapy approaches for effective cancer therapy.

Nanosystem for tumor microenvironment modulation

The complicated tumor microenvironment contains immunosuppressive signals that limit cancer treatment efficacy [98–100]. The common immunosuppressive factors include cytokines, T_{regs}, and TAMs. We will primarily review approaches of functional T cells activation by depletion of these immunosuppressive signals.

Inhibition of immunosuppressive cytokines

Cytokines are small proteins that play a vital role in host immunity. These cytokines are either stimulatory (*e.g.* interferons (IFNs), tumor necrosis factor-α (TNF-α), IL-12, IL-2, IL-1, granulocyte-macrophage colony-stimulating factor (GM-CSF), and C-X-C motif chemokine 10 (CXCL10)) or inhibitory (*e.g.* Fas ligand (FasL), vascular endothelial growth factor (VEGF), transforming growth factor beta (TGF-β), C-X-C motif chemokine 12 (CXCL12), C-X-C motif chemokine 8 (CXCL8)) [101,102]. For example, IFN α is able to affect $CD8^+$ T cells by upregulating MHC I or MHC II in APCs and increase recognition of activated T cells. CXCL12 is the most potent chemokine in promoting angiogenesis and upregulating VEGF in cancer. By inhibiting these immunosuppressive cytokines, we can indirectly activate T cells for immunotherapy. The approaches include targeting DNA/RNA with oligonucleotides or targeting protein with inhibitors. Miao et al. reported that blockade of CXCL12 and PD-L1 molecules by fusion proteins traps could alter immunosuppressive tumor microenvironment and elicit host immune response (Fig. 7a) [46]. They used liposome-protamine-DNA (LPD) nanoparticles, which have low systemic toxicity, long circulation time, and good drug delivery, to encapsulate plasmids encoding CXCL12 and PD-L1 traps. Their results demonstrated that the CXCL12 trap increased T cells penetration into tumors, and that the PD-L1 trap helped to activate tumor infiltrated T cells. In another report, Park et al. used a liposomal nanogel based on cyclodextrins to co-deliver hydrophobic TGF-β inhibitor SB505124 and water

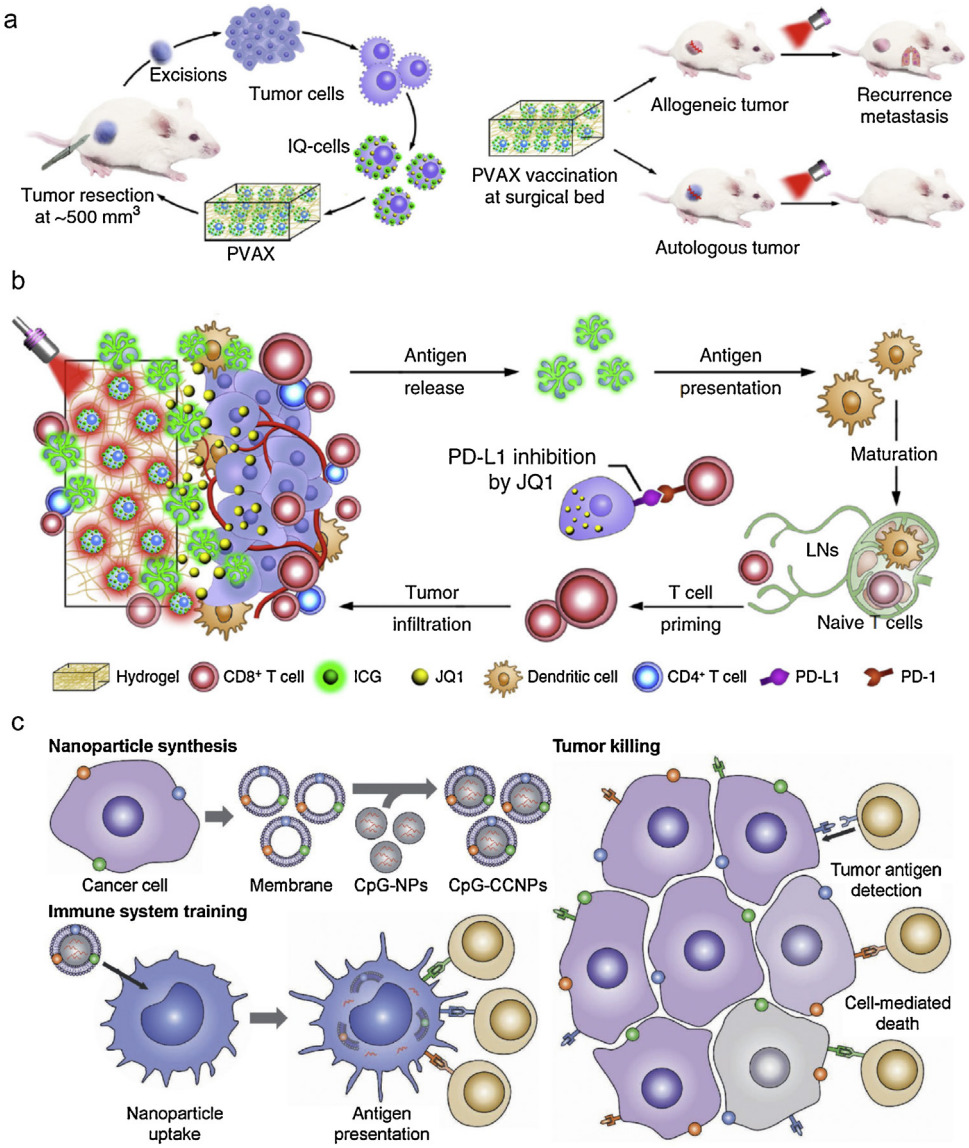

Fig. 6. Schematic illustration of fabrication of PVAX for cancer immunotherapy. (a) Fabrication process of PVAX. (b) Simplified mechanism of PVAX-mediated cancer immunotherapy to prevent post-operative tumor recurrence and metastasis. Adapted from ref. [44] with permission of Nature Publishing Group, Copyright 2018. (c) Schematic of CpG-CCNPs for anticancer vaccination. Adapted from ref. [97] with permission of WILEY-VCH Verlag GmbH & Co. KGaA, Weinheim, Copyright 2017.

soluble IL-2 into the tumor microenvironment for melanoma treatment (Fig. 7b) [47]. The sustained release of the inhibitor and IL-2 significantly inhibited tumor growth, prolonged survival time, improved activity of natural killer cells and increased $CD8^+$ T cells infiltration at tumor site.

Depletion of regulatory T (T_{reg}) cell

Treg cells are immunosuppressive cell that are widely distributed within the tumor microenvironment. They suppress functional T cell response by expressing CD25 (IL-2 receptor), CTLA-4, glucocorticoid-induced TNF receptor (GITR), and C-C chemokine receptor type 4 (CCR4). They also secrete the immunosuppressive cytokine IL-10 [103,104]. Therefore, nanosystems exploiting T_{reg} depletion is a good strategy to promote functional T cell activation, proliferation and elicit host immunity. Cyclophosphamide is an immunosuppressant that preferentially targets T_{reg} cells at low dose [48]. Zhang et al. reported PD-1 presented platelets for PD-L1 blockade with cyclophosphamide encapsulation to deplete Tregs and reinvigoration $CD8^+$ T cells within surgical wound of tumor microenvironment (Fig. 8a, b, c) [48]. Qu et al. developed a combinational immunotherapy based on photoimmunotherapy by IR780 dye and Tregs suppression by inhibitor imatinib (IMT) in glucocorticoid-induced TNF receptor family-related protein (GITR) layer-by-layer hybrid PLGA nanoparticles (LBL hNPs) (Fig. 8d) [105]. IMT is responsible for reducing the activation of STAT3 and STAT5 to inhibit Foxp3 expression. In this manner, Tregs in the microenvironment will become suppressed. Fig. 8e shows the cytotoxicity of LBL hNPs in cellsafter NIR irradiation. Fig. 8f illustrated the down-regulation of Tregs (19.7%) treated by LBL hNPs compared with IMT treatment (30.8%). The authors also found the decrement of $CD4^+$ $Foxp3^+$ T_{reg}s in tumors, which was accompanied by increase GrB and IFN-γ secretion from $CD8^+$ T cells.

Targeting to tumor-associated macrophages (TAMs)

Tumor-associated macrophages (TAMs) are an important population of immune cells in tumor microenvironment [99]. TAMs can be polarized into anti-tumor M1 macrophages (TAMs1) or pro-tumor M2 macrophages (TAMs2). TAMs1 secretes pro-

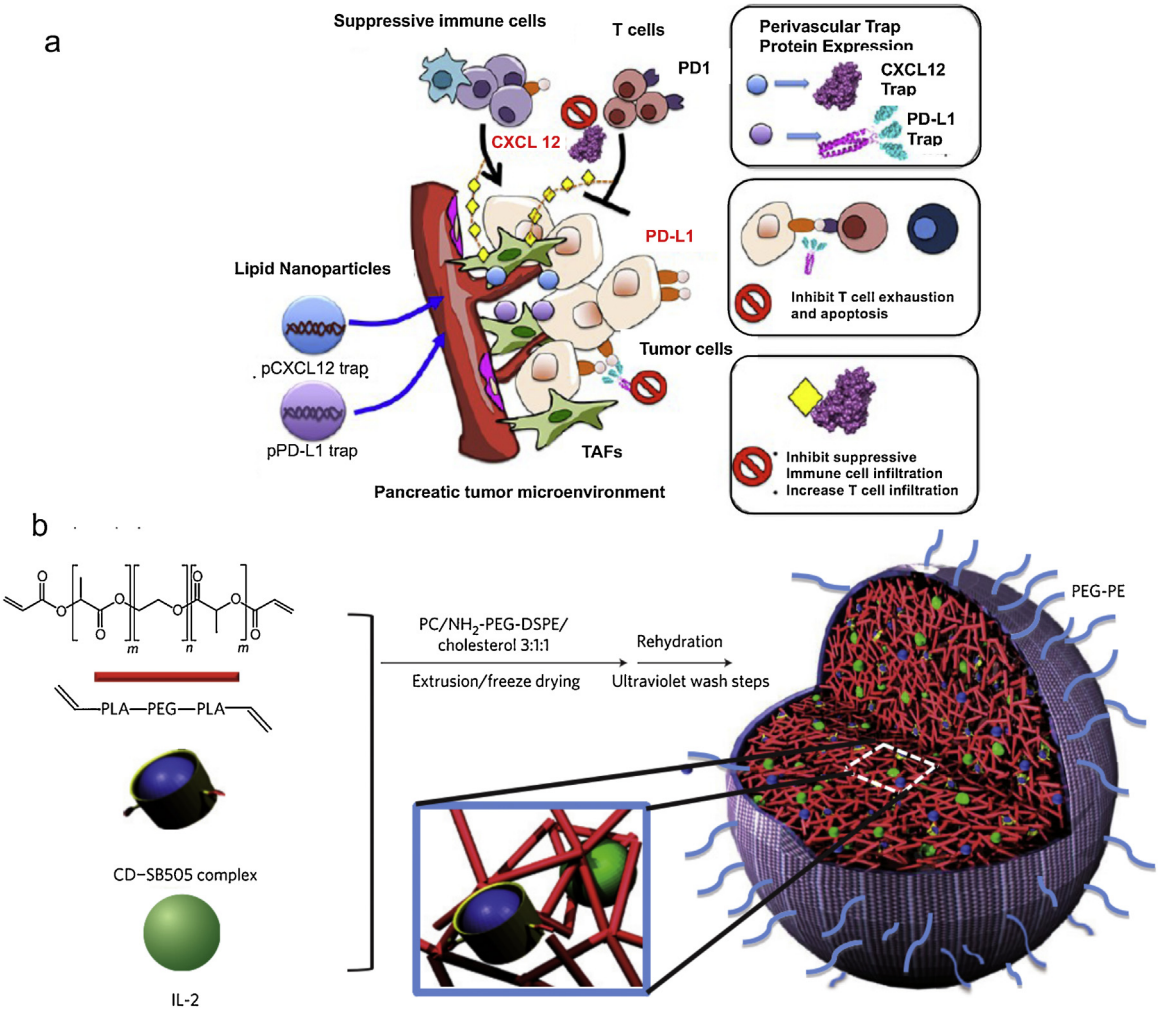

Fig. 7. (a) Mechanism of trap to treat pancreatic cancer. Adapted from ref. [46] with permission of American Chemical Society, Copyright 2017.(b) Fabrication of the nLG particle system. Adapted from ref. [47] with permission of Nature Publishing Group, Copyright 2012.

inflammatory cytokines like TNF-α to enhance anti-tumor effects. TAMs2 can suppress functional T cells by expressing PD-1 and CTLA-4 ligands for TCR and BCR inhibition, by secreting immunosuppressive cytokines (*e.g.*, TGF-β, IL-10), and by depleting L-arginine through arginase secretion to limit expression of CD3 on $CD8^+$ T cells [106]. Over the past few years, research groups have focused on targeting macrophages to improve immunotherapy [107,108]. For example, Qian et al. designed dual targeted nanoparticles by loading anti-colony stimulating factor I receptor (anti-CSF-1R) small interfering RNA to block survival signaling in M2-like macrophage in melanoma xenografts (Fig. 9a) [109]. According to the authors, the nanoparticles demonstrated stronger affinity for M2-like macrophages compared with other macrophages leading to their depletion and tumor growth inhibition. Additionally, according to their results, the siRNA-carrying nanoparticle also down-regulated expression of exhaustion markers (PD-1 and Tim-3) on tumor infiltrating $CD8^+$ T cells and increased secretion of IFN-γ (Fig. 9a). Zhao et al. reported a dual-targeting albumin nanoparticle modified with transferrin receptor (Tfr) binding peptide and mannose to bypass the blood-brain barrier to deliver disulfiram/copper complex to glioma cells [110]. After entry into tumor microenvironment, the particle was able to deliver regorafenib to promote TAMs2 polarization to TAMs1. Remodeling of tumor microenvironment by depletion of TAMs2, Treg cells, activation of $CD8^+$ T cells and/or delivery of effector cytokines conferred anti-glioma efficacy. Shi et al. claimed that they could reprogram TAMs to M1 phenotype using reactive oxygen species (ROS) photogeneration based on mannose-decorated PEGylated PLGA nanoparticles encapsulated with ICG and titanium dioxide (TiO_2). The particles also incorporated ammonium bicarbonate (NH_4HCO_3 or N) for endosome membrane disruption (MAN-PLGA-N) (Fig. 9b) [49]. The MAN-PLGA-N was taken up by macrophages after mannose receptor binding. The loaded NH_4HCO_3 in the particle core was able to generate CO_2 and NH_3 to destabilize endo/lyso membrane leading to ICG and TiO_2 release into the cytoplasm. According to their results, antigen presentation and T-cell priming induced by TAMs was strengthened after inhibition of lysosomal proton pump and proteolytic activity. Fig. 9c show TAMs treated with MAN-PLGA-N had downregulation of the immunosuppressive marker CD206 and upregulation of the anti-tumor molecule iNOS. Finally, the reprogrammed TAMs promoted CTLs recruitment and directed the tumoricidal response by memory T cell. This example illustrates the potential of modifying TAMs as a means to alleviate immune suppression.

Generally speaking, the immunosuppressive factors can promote angiogenesis, express specific receptor (*e.g.*, CD25, PD-1, CTLA-4) on cell surface, or reduce $CD3^+$ expression to indirectly or directly inhibit $CD8^+$ T cell function. Remodeling tumor microenvironment through depletion of immunosuppressive signals (*e.g.*, cytokines, T_{reg}s, TAMs) by nanosystems has been developed as

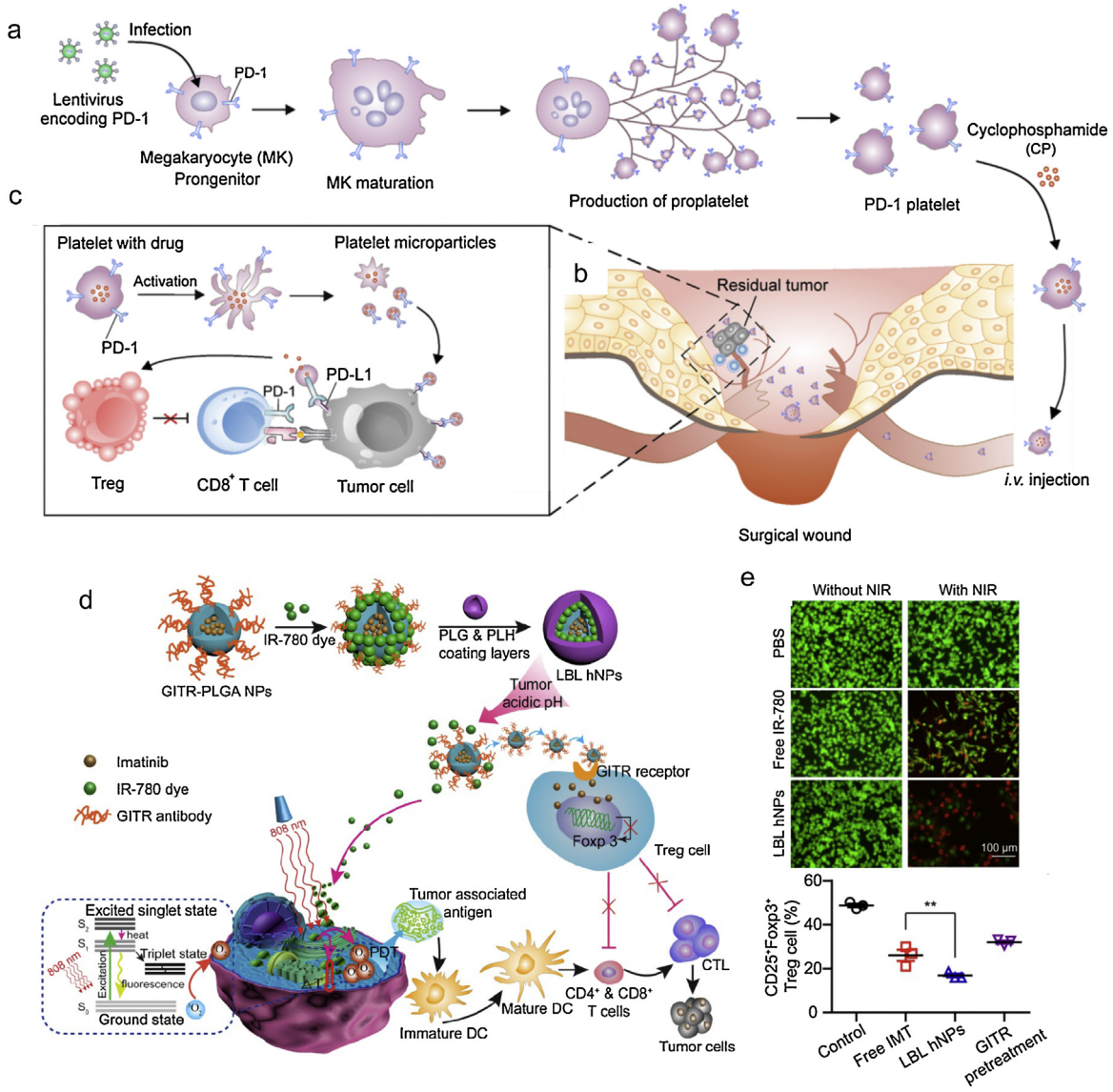

Fig. 8. Schematic of the production of PD-1-expressing platelets and reinvigoration of $CD8^+$ T cells. (a) Schematic shows L8057 cell line stably expressing murine PD-1 and production of platelets. (b) PD-1-expressing platelets target tumor cells within the surgery wound. (c) PD-L1 blockade by PD-1-expressing platelets revert exhausted $CD8^+$ T cells to attack tumor cells. Adapted from ref. [48] with permission of American Chemical Society, Copyright 2018. (d) Schematic illustration of NIR therapy and regulatory T cell modulation using layer-by-layer hybrid nanoparticles (LBL hNPs) with mutual PTT, PDT, and immune-anticancer therapeutic effects. (e) Live and dead cell assay of B16BL/6 cells exposed to different formulations without or with NIR exposure. (f) Effect of different formulations on T_{reg} cell differentiation in the presence of T_{reg} cells and B16BL/6 cells co-culture system. Adapted from ref. [105] with permission of Ivyspring International Publisher, Copyright 2018.

a powerful approach in cancer immunotherapy. Combination of functional T cell activation with immunosuppressive factor depletion by nanosystems will likely have improved antitumor efficacy in cancer immunotherapy.

Nanosystem combination therapy for T cell activation

Owing to tumor heterogeneity, monotherapy is generally difficult to yield satisfactory treatment outcomes. Combination therapy based on multiple therapeutic pathways has become a mainstay in cancer immunotherapy. In the following part, we will summarize the approaches of combinational immunotherapy with chemotherapy, PDT, PTT, and/or RT.

Combination therapy based on chemotherapy

Chemotherapy is generally the first-line therapy for many cancer subtypes. However, it is generally hindered by the severe side effects and unsatisfactory treatment efficacy in clinical practice. Recently, it has been reported that cancer immunotherapy can synergize with chemotherapy. Chemotherapy can lead to immunogenic cell death (ICD) which enhances immunotherapy [111–115]. For example, Lu et al. reported a nanosystem that enabled the induction of ICD and inhibition of indoleamine-pyrrole 2,3-dioxygenase (IDO) immunosuppressive signaling in pancreatic ductal adenocarcinoma (PDAC) (Fig. 10a) [114]. In their system, they used oxaliplatin as the ICD-inducing chemotherapeutic agent and indoximod (IND) as the IDO inhibitor. According to the authors, this class of drug and inhibitor loaded nanoparticles can produce robust immune response by activating both innate and adaptive immune system after local or intravenous injection in an orthotopic pancreatic tumor model. According to their results, the tumor was eradicated because of the recruitment of cytotoxic T lymphocytes in tumor site and the depletion of immunosuppressive $Foxp3^+$ T cells. Song et al. used two chitosan derivatives with opposite charges to prepare tumor microenvironment responsive nanogel

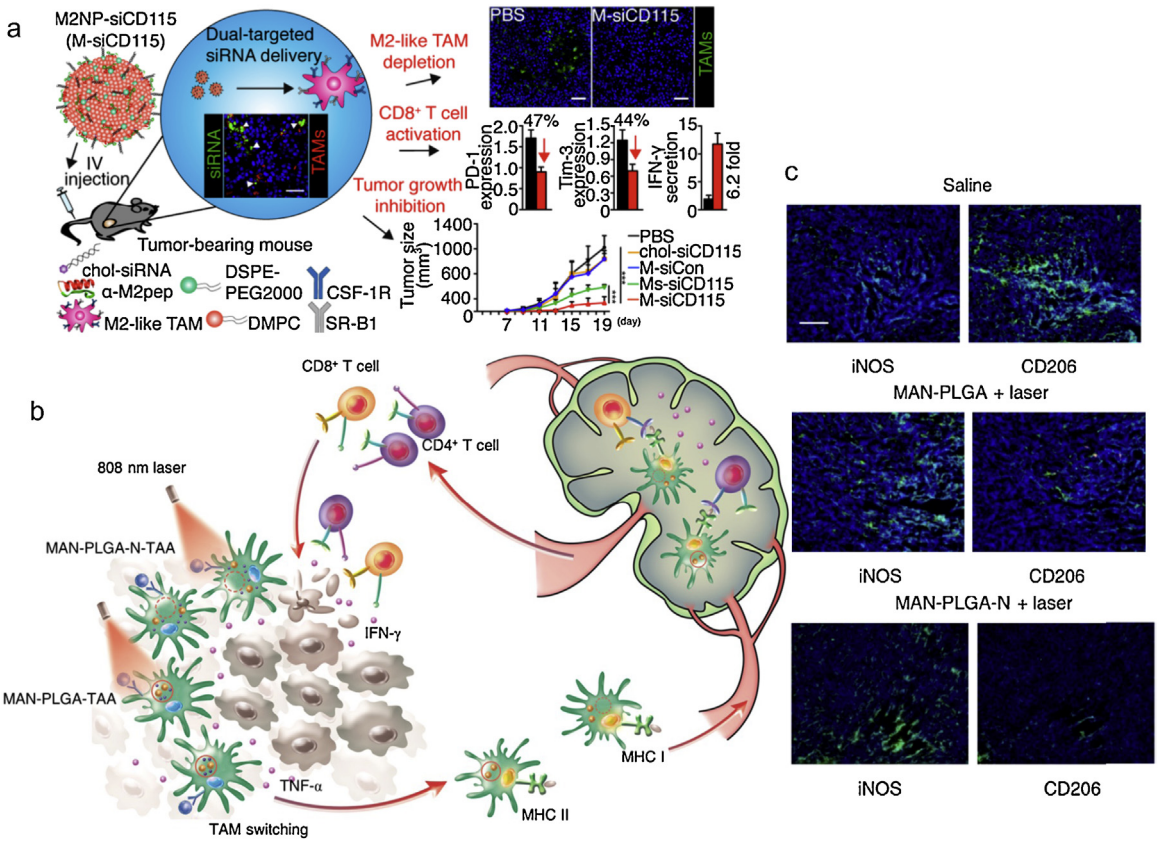

Fig. 9. (a) Design of the M2NP for M2-like TAM-specific molecular-targeted immunotherapy and in vivo antitumor efficacy. Adapted from ref. [109] with permission of American Chemical Society, Copyright 2017. (b) Schematic of TAM-directed cancer immunotherapy with nanoparticle-based ROS photogeneration. (c) Immunostaining of the expression of M1 and M2 markers in TAMs of tumors intravenously treated with MAN-PLGA or MAN-PLGA-N nanoparticles with or without laser illumination. MAN and N in MAN-PLGA-N represent mannose and ammonium bicarbonate, respectively. Adapted from ref. [49] with permission of American Chemical Society, Copyright 2018.

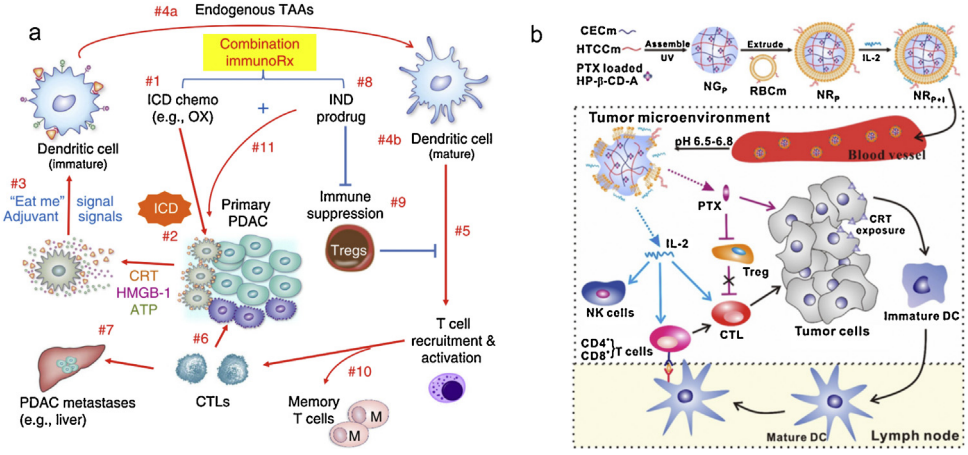

Fig. 10. (a) Schematic illustration that how dual delivery of OX and IND may impact the anti-PDAC immune response. Adapted from ref. [114] with permission of Nature Publishing Group, Copyright 2017. (b) Preparation of NRP+I and schematic illustration of chemo-immunotherapy. Adapted from ref [55]. with permission of American Chemical Society, Copyright 2017.

modified with erythrocyte membrane (Fig. 10b) [55]. After loading the ICD-inducing agent paclitaxel and cytokine IL-2, their results showed that release of the two drugs caused calreticulin exposure, increment of cytotoxic T cells infiltration and decrement of immunosuppressive factors. Liu et al. exploited tumor microenvironment responsive nanocarrier to co-deliver mitoxantrone (MIT) and celastrol (CEL) with an optimal ratio (5:1) for synergistic ICD with good antitumor effect in desmoplastic melanoma [116]. They found that the synergy between the two chemotherapeutic drugs required less drug dose which can lower possible side effects.

Wang et al. developed a chemoimmunotherapy approach via controlled release of gemcitabine (GEM) and anti-PD-L1 by ROS-responsive scaffold gel (GEM@Gel) [115]. They found that low dose GEM could induce cell death, up-regulate PD-L1 expression in surviving tumor cell population, and inhibit myeloid-derived suppressor cell (MDSCs) for effector T cell activation. They also

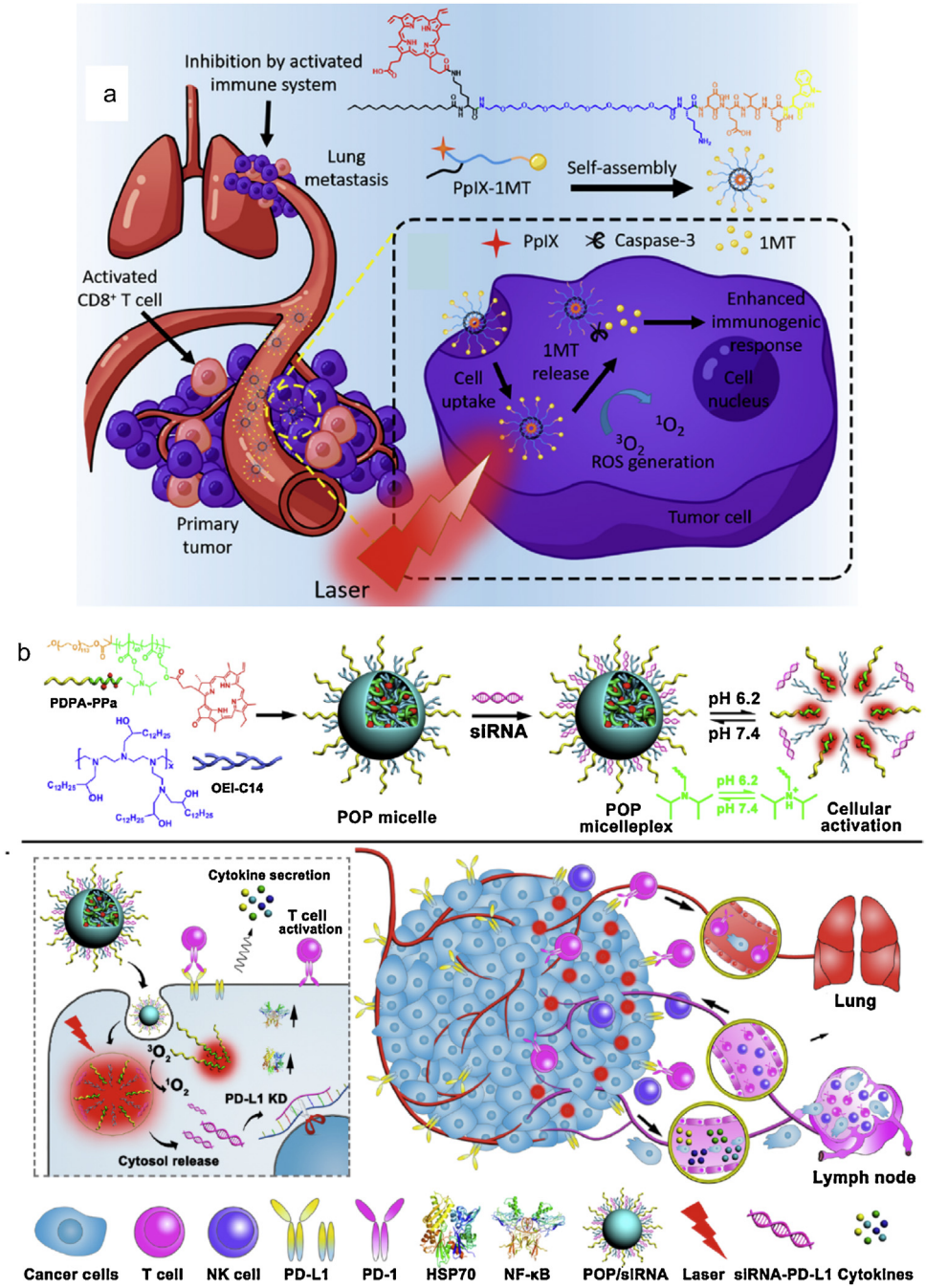

Fig. 11. (a) Structure of the chimeric peptide PpIX-1 MT, as well as *in situ* PDT in the primary tumor caused apoptosis of tumor cells, production of caspase-3, and release of 1 MT from PpIX-1 MT nanoparticles. Adapted from ref. [123] with permission of American Chemical Society, Copyright 2018. (b) Self-assembly of POP micelleplex and cartoon schematic of POP-PD-L1 micelleplex mediated photodynamic cancer immunotherapy. Adapted from ref. [125] with permission of American Chemical Society, Copyright 2016.

claimed that GEM@Gel promoted T cell infiltration, TAMs polarization with impressive 4T1 and B16F10 tumor growth inhibition when combined with checkpoint blockade by anti-PD-L1.

Combination therapy built on photodynamic therapy (PDT)

Photodynamic therapy (PDT) can generate ROS and induce tumor necrosis and apoptosis after laser irradiation [117–119]. In turn, the deceased tumor cells will release TAAs which can be captured by DCs and promote DCs maturation. The mature DCs migrate to lymph node and activate cytotoxic T lymphocytes for immune response [120]. However, PDT alone might not be able to completely kill tumor cells because of the immunosuppressive tumor microenvironment. Many studies have shown enhanced cancer immunotherapy efficacy because of PDT [121–124]. Dai et al. reported size/charge tunable pH-responsive micelleplex for PDT enhanced PD-L1 immunotherapy with good tumor penetration [121]. The micellar nanocomplex delivered siRNA to silence PD-L1 and photosensitizer to target mitochondria for synergistic PDT/immunotherapy. After release of siRNA and photosensitizer, the nanosystems enhanced immune response by PDT and checkpoint blockade for T cells activation. This led to inhibition of melanoma tumor growth and recurrence. He et al. developed core-shell nanoparticles by loading

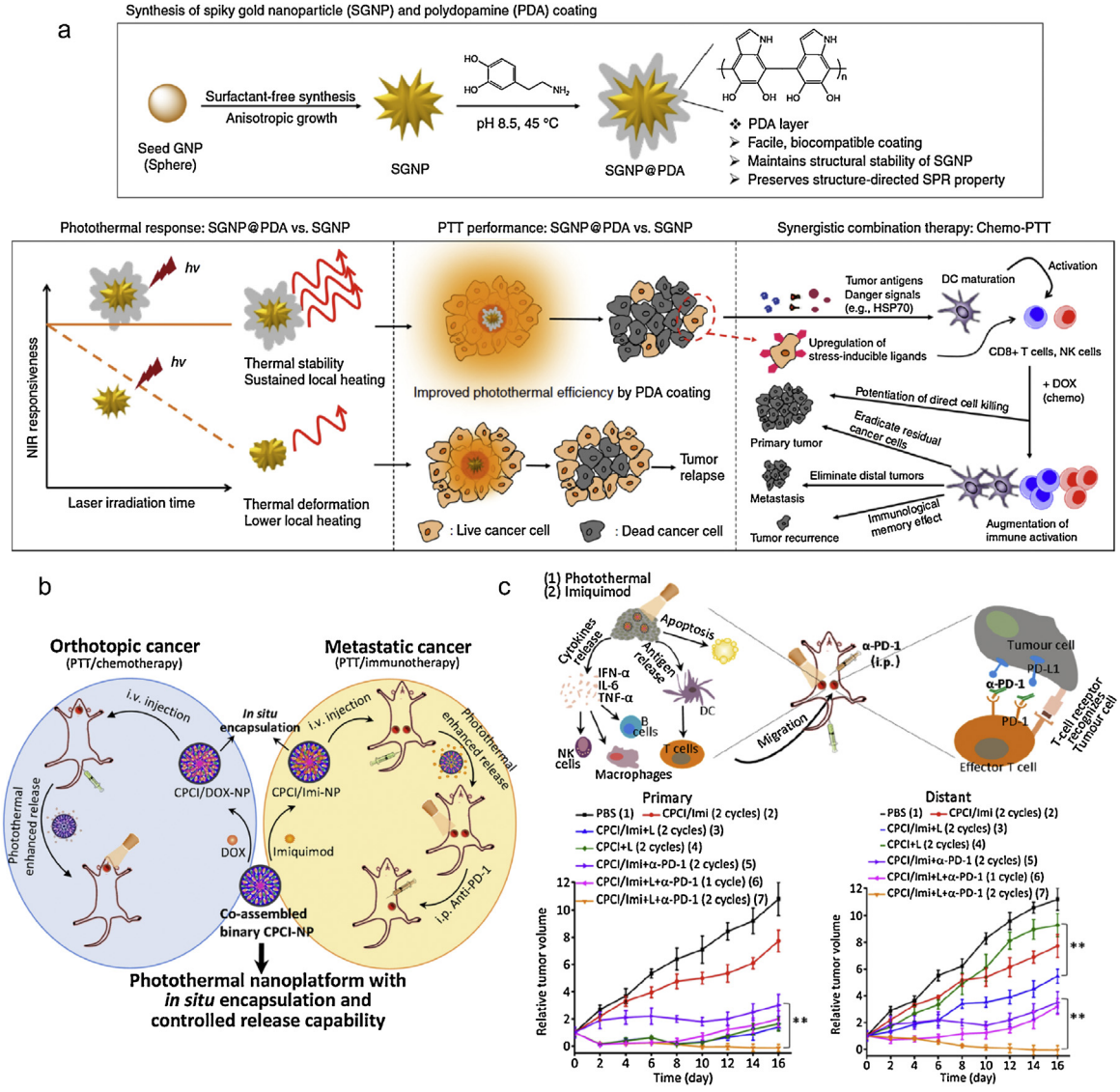

Fig. 12. (a) The schematic illustration shows the development of spiky gold nanoparticles (SGNPs) coated with PDA (SGNP@PDA) as a new photothermal agent with extensive photothermal stability and efficiency. Adapted from ref. [128] with permission of Nature Publishing Group, Copyright 2018. (b) Schematic illustration of high-performance photothermal nanoparticle (CPCI-NP). (c) Synergistic antitumor activity of photothermal/immunotherapy in the mice bearing orthotopic 4T1 breast cancer (both sides). Adapted from ref. [129] with permission of American Chemical Society, Copyright 2018.

the chemotherapeutic drug oxaliplatin in the core for ICD and photosensitizer pyropheophorbide-lipid conjugate in the shell for PDT [122]. In combination with anti-PD-L1, their results indicated the stronger T cell mediated response with corresponding colon tumor regression. Song et al. synthesized chimaeric peptide C16-K(PpIX)-PEG8-KDEVD-1 MT (PpIX-1 MT) which contains the photosensitizer protoporphyrin (PpIX) for PDT and the IDO inhibitor 1-methyltryptophan (1 MT). 1 MT was placed at the C-terminus of the sequence behind a caspase-3 responsive sequence (Fig. 11a) [123]. The authors postulated that PpIX-1 MT could induce ROS generation after laser irradiation. Once the affected cancer cells will undergo apoptosis, they will express caspase-3 and facilitate 1 MT release. IDO inhibition is then expected to enhance immune response and $CD8^+$ T cells activation. Wang et al. constructed a versatile micelleplex composed of pH sensitive micelle, siRNA for knocking down PD-L1 expression and photosensitizer pheophorbide A (PPa) for PDT (Fig. 11b) [125]. They found that combinational therapy of PDT and PD-L1 knockdown increased $CD4^+$, $CD8^+$ T cells, as well as TNF-α and IFN-γ dual positive $CD8^+$ T cell in tumor site. In addition, they also claimed that the combination therapy improved anti-tumor efficacy and inhibited distant tumor metastasis in B16F10 melanoma model.

Combination therapy based on photothermal therapy (PTT)

Photothermal therapy is an efficient cancer immunotherapy approach by using vibrational energy (heat) from laser irradiation to induce tumor cell death. However, it is difficult to achieve complete elimination of tumor cells with PTT alone. Combination therapy between PTT and other approaches (*e.g.*, chemotherapy, PDT) has shown promise especially for some disseminated tumor models [126–129]. Research by Nam et al. revealed that PTT combined with chemotherapy triggered robust anti-tumor immune response in disseminated tumors (Fig. 12a) [128]. They utilized gold nanoparticles as photothermal agents decorated with polydopamine on the outer surface to increase stability and efficiency of the NIR response. According to their results, combination therapy with doxorubicin displayed improved anti-tumor immunity and prominent inhibition for the both primary and distant tumor in the CT26 colon carcinoma model. The nanoparticles were also effective

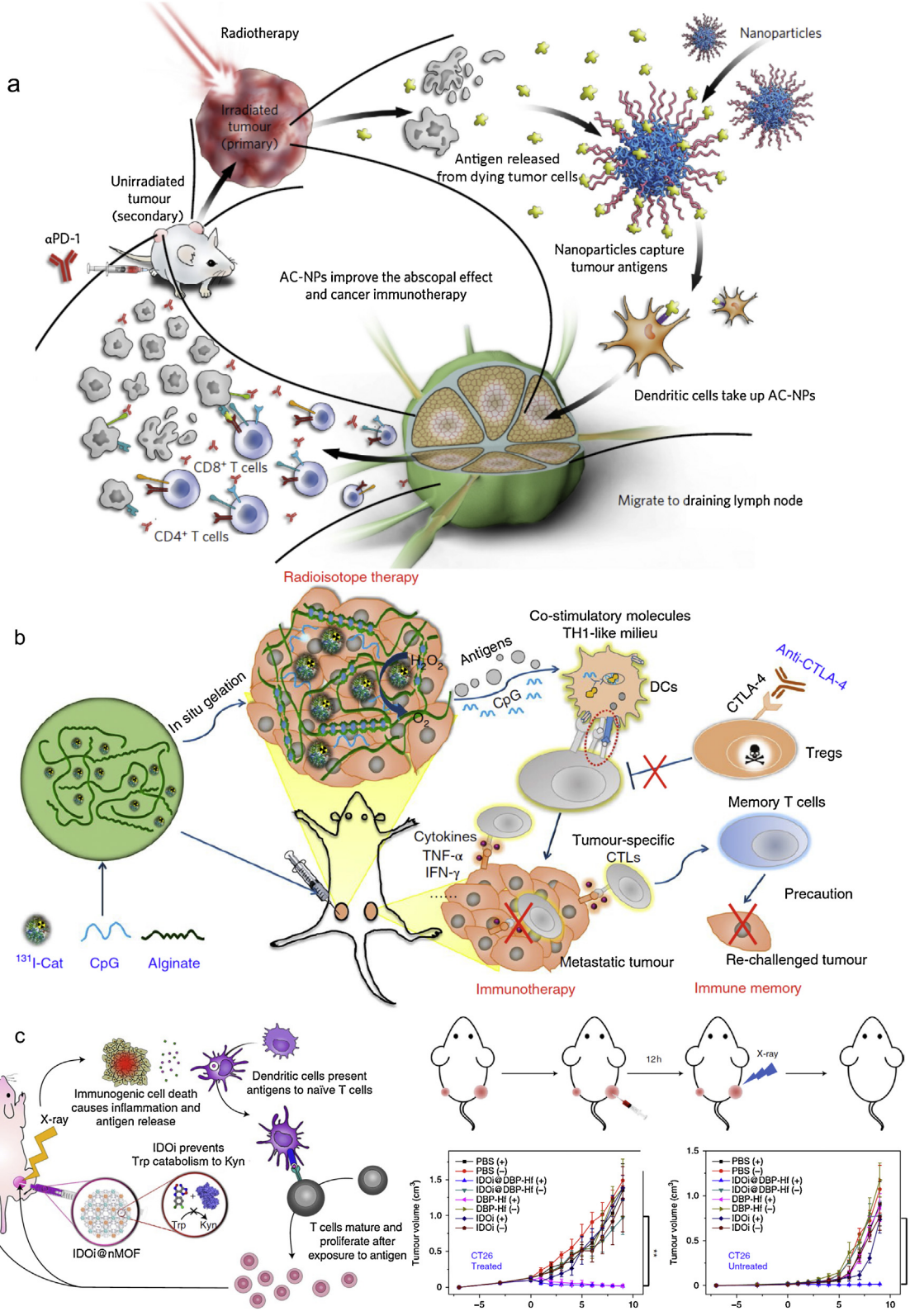

Fig. 13. (a) Schematic depiction of utilizing AC-NPs to improve cancer immunotherapy. Adapted from ref. [130] with permission of Nature Publishing Group, Copyright 2017. (b) Mechanism of anti-tumor immune responses induced by ^{131}I-Cat/CpG/ALG-based RIT in combination with checkpoint blockade. Adapted from ref. [132] with permission of Nature Publishing Group, Copyright 2018. (c) nMOFs enable synergistic RT-RDT and immunotherapy using extremely low doses of X-rays in CT26 tumor model. Adapted from ref. [133] with permission of Nature Publishing Group, Copyright 2018.

in the TC-1 submucosa-lung metastasis tumor model. The results were attributed to activation and infiltration of CD 8$^+$ T cells and NK cells. Peng et al. reported the use of NLG919/IR780 micelles for PTT combination therapy with IDO inhibition [126]. The expression of immunosuppressive factors, like IDO, heat shock protein (HSP) and programmed death ligand-1 (PD-L1) can also reduce PTT efficacy. Notably, their results demonstrated that NLG919/IR780 micelles for the combination therapy were able to reduce IDO activity, inhibit

primary tumor growth, and promote cytotoxic T lymphocytes activation for treatment of distant tumors. Zhang et al. reported a hybrid CPCI-NP derived from the co-self-assembly of two telodendrimers PEG5K-CA4-ICGD4 (PCI) and PEG5K-Cys4-L8-CA8 (PCLC) [129]. They proved that CPCI-NP had efficient antitumor activity in orthotopic OSC-3 oral cancer model when combined with PTT/chemotherapeutic therapy using ICG and DOX (Fig. 12b). They further verified that CPCI-NP co-loaded with ICG and immunomodulatory molecule imiquimod displayed superior inhibition efficacy against 4T1 tumor model, especially when PTT/immuno-therapy was combined with anti- PD-1 checkpoint blockade (Fig. 12b&c).

Combination therapy built on radiotherapy (RT)

Radiotherapy (RT) uses ionization energy to kill cancer cells. However, radiation delivered to normal tissues is the main limitation of this approach. Many studies have shown that radiotherapy can also elicit host immunity for immunotherapy based on the abscopal effect [130,131]. At high doses, there are concerns for radiation toxicity to normal tissues. At low doses, tumors may be undertreated. Combining RT with other approaches (*e.g.*, chemotherapy, checkpoint blockade therapy) may help to address dosing issues [130,132,133]. Min et al. reported nanoparticles with specific moieties (*e.g.*, amine, 1,2-dioleoyloxy-3-(trimethylammonium)propane, maleimide (Mal)) that could capture antigens for improved antigen presenting and enhanced immunity response after RT combined with immune checkpoint blockade (Fig. 13a) [130]. In B16-F10 melanoma carcinoma model, a 20% cure rate was achieved with the combination while no mice were cured in the control group. According to the authors, the expansion of CD 8^+ T cells was the primary reason for tumor growth inhibition after combination therapy. Chao et al. designed combinational therapy using local radionuclide therapy together with anti-CTLA-4 immune checkpoint blockade (Fig. 13b) [132]. They claimed that catalase labeled with ^{131}I can attenuate level of hypoxia in tumors and potentiated RT efficacy at low radioactive dose. Moreover, after injection, hydrogel formation upon exposure to endogenous Ca^+ helped to fix ^{131}I within the tumor. The formulation combined with CpG and anti-CTLA-4 was able to inhibit tumor metastasis and subsequent rechallenge due to the activation and infiltration of CD 8^+ T cells. In another report, Lu et al. exploited nanoscale metal-organic framework (nMOF) for radiotherapy-radiodynamic therapy combination with IDO inhibitor for $CD8^+$ T cells maturation and proliferation (Fig. 13c) [133]. They claimed that nMOF could eradicate both local and distant breast and colorectal tumors after intratumoral injection of the nMOF encapsulated with IDOi under low-dose X-ray irradiation.

Conclusions and outlook

In recent years, nanosystems-based cancer immunotherapy for functional T cell activation has gained great momentum. As we discussed in this review, every approach has its own pros and cons. Nanoparticle-based aAPCs could mimic APCs to directly elicit T cell responses in lymph nodes and provoke host's immune response. This method obviates the need to harvess APCs, stimulate antigen processing and presentation *ex vivo*, and refuse into host. Compared with bispecific T-cell engaging antibodies (BiTEG), which can directly kill cancer cells by specfic antigen recognition with perforin and granzyme secretion [134], aAPCs need to first activate T cells to induce cell death. Cancer nanovaccine can efficiently deliver TAAs, neoantigen, adjuvant to lymph node, or form cancer vaccination *in vitro* and *in vivo* for functional T cell activation. Their flexible design enables affords a multitude of combination. Nevertheless, nanovaccine delivery systems will most likely require mutiple administrations for prolonged immune response. TME modulation mediated by nanoparticles is able to reinvigorate $CD8^+$ T cells, $CD4^+$ T cells, effector T cells and increase survival rate of memory T cells. This helps to counteract tumor evasion from immune surveillance.

Unlike monotherapy, combination therapy can better cope with immune resistance and appear to be the trend of future cancer immunotherapy. For instance, future cancer nanovaccines may one day be able to simulataneously prime and active T cells, modulate tumor microenvironment and inhibit negative regulatory signals. In this review, we mainly focused our discussion on therapeutic approaches regarding cancer immunotherapy for functional T cell activation. In clinical setting, diagnostic information is necessary to provide guidelines for cancer treatment. In this respect, molecular imaging modalities (*e.g.*, positron emission tomography (PET), single-photon emission computerized tomography (SPECT), magnetic resonance imaging (MRI)) can be used [135,136]. Combining nanomedine-based diagnosis and therapy, nanoimmunotheranostics, will probably emerge as one of the research hotspots in future.

Even though nanosystem-based immunotheranostics are promising, there are still inevitable obstacles to overcome prior to clinical translation. Simplification of synthesis process is necessary to decrease the use of organic solvent, and to ensure product purity. The cooperativity (*e.g.*, doses, categories) between immunotherapeutic drugs and diagnostic agents will play a key role in achieving satisfactory treatment efficacy. In addition, the long term safety of nanomaterials must be carefully assessed especially for potential autoimmune reponses. Ultimately, accurate diagnosis combined with effective immunotherapy will greatly improve outcomes for cancer patients.

Acknowledgements

This work was supported by the Intramural Research Program (IRP) of the National Institute of Biomedical Imaging and Bioengineering (NIBIB), National Institutes of Health (NIH) and National Natural Science Foundation of China (NSFC 81471689, 81771873 and 91859207).

References

[1] J.C. Frankel, Science 342 (2013) 1432–1433.
[2] A. Domling, T.A. Holak, Angew Chem. Int. Ed. 53 (2014) 2286–2288.
[3] K.C. Ohaegbulam, A. Assal, E. Lazar-Molnar, Y. Yao, X. Zang, Trends Mol. Med. 21 (2015) 24–33.
[4] O. Hamid, C. Robert, A. Daud, F.S. Hodi, W.J. Hwu, R. Kefford, et al., N. Engl. J. Med. 369 (2013) 134–144.
[5] E.B. Garon, N.A. Rizvi, R. Hui, N. Leighl, A.S. Balmanoukian, J.P. Eder, et al., N. Engl. J. Med. 372 (2015) 2018–2028.
[6] D.M. Pardoll, Nat. Rev. Cancer 12 (2012) 252–264.
[7] A. Snyder, V. Makarov, T. Merghoub, J. Yuan, J.M. Zaretsky, A. Desrichard, et al., N. Engl. J. Med. 371 (2014) 2189–2199.
[8] S.L. Maude, N. Frey, P.A. Shaw, R. Aplenc, D.M. Barrett, N.J. Bunin, et al., N. Engl. J. Med. 371 (2014) 1507–1517.
[9] A.D. Fesnak, C.H. June, B.L. Levine, Nat. Rev. Cancer 16 (2016) 566–581.
[10] S.A. Grupp, M. Kalos, D. Barrett, R. Aplenc, D.L. Porter, S.R. Rheingold, et al., N. Engl. J. Med. 368 (2013) 1509–1518.
[11] S.A. Rosenberg, N.P. Restifo, J.C. Yang, R.A. Morgan, M.E. Dudley, Nat. Rev. Cancer 8 (2008) 299–308, fet[11].
[12] N.P. Restifo, M.E. Dudley, S.A. Rosenberg, Nat. Rev. Immunol. 12 (2012) 269–281.
[13] J. Banchereau, A.K. Palucka, Nat. Rev. Immunol. 5 (2005) 296–306.
[14] Z. Hu, P.A. Ott, C.J. Wu, Nat. Rev. Immunol. 18 (2018) 168–182.
[15] J. Banchereau, K. Palucka, Nat. Rev. Clin. Oncol. 15 (2018) 9–10.
[16] M.A. Cheever, C.S. Higano, Clin. Cancer Res. 17 (2011) 3520–3526.
[17] M.R. Junttila, F.J. de Sauvage, Nature 501 (2013) 346–354.
[18] C.G. Drake, E.J. Lipson, J.R. Brahmer, Nat. Rev. Clin. Oncol. 11 (2014) 24–37.
[19] C.S. Hinrichs, N.P. Restifo, Nat. Biotechnol. 31 (2013) 999–1008.
[20] W. Zou, Nat. Rev. Cancer 5 (2005) 263–274.
[21] T.F. Gajewski, H. Schreiber, Y.X. Fu, Nat. Immunol. 14 (2013) 1014–1022.
[22] S.D. Jo, G.-H. Nam, G. Kwak, Y. Yang, I.C. Kwon, Nano Today 17 (2017) 23–37.
[23] C. Wang, Y. Ye, Q. Hu, A. Bellotti, Z. Gu,Adv. Mater. 29 (2017), 1606036.
[24] C.H. Kapadia, J.L. Perry, S. Tian, J.C. Luft, J.M. DeSimone, J. Control. Release 219 (2015) 167–180.

[25] H. Wang, D.J. Mooney, Nat. Mater. 17 (2018) 761–772.
[26] L.J. Eggermont, L.E. Paulis, J. Tel, C.G. Figdor, Trends Biotechnol. 32 (2014) 456–465.
[27] C. Wang, W. Sun, Y. Ye, H.N. Bomba, Z. Gu, Theranostics 7 (2017) 3504–3516.
[28] K. Palucka, J. Banchereau, Nat. Rev. Cancer 12 (2012) 265–277.
[29] I. Melero, G. Gaudernack, W. Gerritsen, C. Huber, G. Parmiani, S. Scholl, et al., Nat. Rev. Clin. Oncol. 11 (2014) 509–524.
[30] C.G. Figdor, I.J. de Vries, W.J. Lesterhuis, C.J. Melief, Nat. Med. 10 (2004) 475–480.
[31] I. Mellman, G. Coukos, G. Dranoff, Nature 480 (2011) 480–489.
[32] B. Ding, S. Shao, C. Yu, B. Teng, M. Wang, Z. Cheng, et al.,Adv. Mater. (2018), 1802479.
[33] G. Zhu, F. Zhang, Q. Ni, G. Niu, X. Chen, ACS Nano 11 (2017) 2387–2392.
[34] M. Luo, H. Wang, Z. Wang, H. Cai, Z. Lu, Y. Li, et al., Nat. Nanotechnol. 12 (2017) 648–654.
[35] L. Qiu, M. Valente, Y. Dolen, E. Jager, M.T. Beest, L. Zheng, et al.,Small 14 (2018), 1703539.
[36] R. Kuai, L.J. Ochyl, K.S. Bahjat, A. Schwendeman, J.J. Moon, Nat. Mater. 16 (2017) 489–496.
[37] M. Luo, L.Z. Samandi, Z. Wang, Z.J. Chen, J. Gao, J. Control. Release 263 (2017) 200–210.
[38] M.S. Goldberg, Cell 161 (2015) 201–204.
[39] J. Shi, P.W. Kantoff, R. Wooster, O.C. Farokhzad, Nat. Rev. Cancer 17 (2017) 20–37.
[40] Q. He, S. Guo, Z. Qian, X. Chen, Chem. Soc. Rev. 44 (2015) 6258–6286.
[41] C. Liang, L. Xu, G. Song, Z. Liu, Chem. Soc. Rev. 45 (2016) 6250–6269.
[42] X.X. Zhang, H.S. Eden, X. Chen, J. Control. Release 159 (2012) 2–13.
[43] Q. Chen, L. Xu, C. Liang, C. Wang, R. Peng, Z. Liu, Nat. Commun. 7 (2016) 13193.
[44] T. Wang, D. Wang, H. Yu, B. Feng, F. Zhou, H. Zhang, et al., Nat. Commun. 9 (2018) 1532.
[45] D.J. Irvine, M.C. Hanson, K. Rakhra, T. Tokatlian, Chem. Rev. 115 (2015) 11109–11146.
[46] L. Miao, J. Li, Q. Liu, R. Feng, M. Das, C.M. Lin, et al., ACS Nano 11 (2017) 8690–8706.
[47] J. Park, S.H. Wrzesinski, E. Stern, M. Look, J. Criscione, R. Ragheb, et al., Nat. Mater. 11 (2012) 895–905.
[48] X. Zhang, J. Wang, Z. Chen, Q. Hu, C. Wang, J. Yan, et al., Nano Lett. 18 (2018) 5716–5725.
[49] C. Shi, T. Liu, Z. Guo, R. Zhuang, X. Zhang, X. Chen, Nano Lett. 18 (2018) 7330–7342.
[50] J. Liu, Q. Chen, L. Feng, Z. Liu, Nano Today 21 (2018) 55–73.
[51] C. von Roemeling, W. Jiang, C.K. Chan, I.L. Weissman, B.Y. Kim, Trends Biotechnol. 35 (2017) 159–171.
[52] L. Tang, X. Yang, Q. Yin, K. Cai, H. Wang, I. Chaudhury, et al., Proc. Natl. Acad. Sci. U. S. A. 111 (2014) 15344–15349.
[53] M.O. Durymanov, A.A. Rosenkranz, A.S. Sobolev, Theranostics 5 (2015) 1007–1020.
[54] W. Fan, B. Yung, P. Huang, X. Chen, Chem. Rev. 117 (2017) 13566–13638.
[55] Q. Song, Y. Yin, L. Shang, T. Wu, D. Zhang, M. Kong, et al., Nano Lett. 17 (2017) 6366–6375.
[56] Y. Liu, P. Bhattarai, Z. Dai, X. Chen, Chem. Soc. Rev. (2018), http://dx.doi.org/10.1039/c1038cs00618k.
[57] A.J. Moy, J.W. Tunnell, Adv. Drug Deliv. Rev. 114 (2017) 175–183.
[58] M. Oelke, C. Krueger, R.L. Giuntoli 2nd, J.P. Schneck, Trends Mol. Med. 11 (2005) 412–420.
[59] J.C. Sunshine, K. Perica, J.P. Schneck, J.J. Green, Biomaterials 35 (2014) 269–277.
[60] E.R. Steenblock, S.H. Wrzesinski, R.A. Flavell, T.M. Fahmy, Expert Opin. Biol. Ther. 9 (2009) 451–464.
[61] J.V.D. Weijden, L.E. Paulis, M. Verdoes, J.C.M.V. Hest, C.G. Figdor, Chem. Sci. 5 (2014) 3355–3367.
[62] A.K. Kosmides, R.A. Meyer, J.W. Hickey, K. Aje, K.N. Cheung, J.J. Green, et al., Biomaterials 118 (2017) 16–26.
[63] E.R. Steenblock, T.M. Fahmy, Mol. Ther. 16 (2008) 765–772.
[64] B. Chen, Y. Jia, Y. Gao, L. Sanchez, S.M. Anthony, Y. Yu, ACS Appl. Mater. Inter. 6 (2014) 18435–18439.
[65] A.S. Cheung, D.K.Y. Zhang, S.T. Koshy, D.J. Mooney, Nat. Biotechnol. 36 (2018) 160–169.
[66] R.A. Meyer, J.C. Sunshine, K. Perica, A.K. Kosmides, K. Aje, J.P. Schneck, et al., Small 11 (2015) 1519–1525.
[67] F. TR, S. ER, S. E, L. N, W. X, H. GL, et al., Nano Lett. 8 (2008) 2070-2076.
[68] S. Mandal, Z.H. Eksteen-Akeroyd, A.J.A. Lambeck, J.C.M.V. Hest, K. Blank, A.E. Rowan, et al., Chem. Sci. 4 (2013) 4168–4174.
[69] K. Perica, A. Tu, A. Richter, J.G. Bieler, M. Edidin, J.P. Schneck, ACS Nano 8 (2014) 2252–2260.
[70] C.S. Chiang, Y.J. Lin, R. Lee, Y.H. Lai, H.W. Cheng, C.H. Hsieh, et al., Nat. Nanotechnol. 13 (2018) 746–754.
[71] G. Zhu, G.M. Lynn, O. Jacobson, K. Chen, Y. Liu, H. Zhang, et al., Nat. Commun. 8 (2017) 1954.
[72] C. Wang, P. Li, L. Liu, H. Pan, H. Li, L. Cai, et al., Biomaterials 79 (2016) 88–100.
[73] P. Zhang, Y.-C. Chiu, L.H. Tostanoski, C.M. Jewell, ACS Nano 9 (2015) 6465–6477.
[74] X. Li, A.M. Aldayel, Z. Cui, J. Control. Release 173 (2014) 148–157.
[75] K.T. Mody, A. Popat, D. Mahony, A.S. Cavallaro, C. Yu, N. Mitter, Nanoscale 5 (2013) 5167–5179.
[76] R.H. Fang, C.M. Hu, B.T. Luk, W. Gao, J.A. Copp, Y. Tai, et al., Nano Lett. 14 (2014) 2181–2188.
[77] K.S. Kim, H. Kim, Y. Park, W.H. Kong, S.W. Lee, S.J. Kwok, et al., Adv. Funct. Mater. 26 (2016) 2512–2522.
[78] S.T. Reddy, A.J. van der Vlies, E. Simeoni, V. Angeli, G.J. Randolph, C.P. O'Neil, et al., Nat. Biotechnol. 25 (2007) 1159–1164.
[79] E.A. Scott, A. Stano, M. Gillard, A.C. Maio-Liu, M.A. Swartz, J.A. Hubbell, Biomaterials 33 (2012) 6211–6219.
[80] R. Yang, J. Xu, L. Xu, X. Sun, Q. Chen, Y. Zhao, et al., ACS Nano 12 (2018) 5121–5129.
[81] R. Kuai, X. Sun, W. Yuan, L.J. Ochyl, Y. Xu, A. Hassani Najafabadi, et al., J. Control. Release 282 (2018) 131–139.
[82] Y. Chu, Q. Liu, J. Wei, B. Liu, Theranostics 8 (2018) 4238–4246.
[83] F. Steinhagen, T. Kinjo, C. Bode, D.M. Klinman, Vaccine 29 (2011) 3341–3355.
[84] A. Pashine, N.M. Valiante, J.B. Ulmer, Nat. Med. 11 (2005) S63–68.
[85] P. Nikolai, A. Julio César, Immunol. Cell Biol. 82 (2004) 488–496.
[86] C.A. Shaw, M.S. Petrik, J. Inorg. Biochem. 103 (2009) 1555–1562.
[87] S.L. Hem, H. Harm, Expert Rev. Vaccines 6 (2007) 685.
[88] G. Zhu, L. Mei, H.D. Vishwasrao, O. Jacobson, Z. Wang, Y. Liu, et al., Nat. Commun. 8 (2017) 1482.
[89] A.W. Li, M.C. Sobral, S. Badrinath, Y. Choi, A. Graveline, A.G. Stafford, et al., Nat. Mater. 17 (2018) 528–534.
[90] F.A. Sharp, D. Ruane, B. Claass, E. Creagh, J. Harris, P. Malyala, et al., Proc. Natl. Acad. Sci. U. S. A. 106 (2009) 870–875.
[91] Y. Xia, J. Wu, W. Wei, Y. Du, T. Wan, X. Ma, et al., Nat. Mater. 17 (2018) 187–194.
[92] A. Sinha, B. Cha, Y. Choi, T. Nguyen, P. Yoo, J. Jeong, et al., Chem. Mater. 29 (2017) 6883–6892.
[93] C. Guo, M.H. Manjili, J.R. Subjeck, D. Sarkar, P.B. Fisher, X.Y. Wang, Adv. Cancer Res. 119 (2013) 421–475.
[94] L. Luo, C. Zhu, H. Yin, M. Jiang, J. Zhang, B. Qin, et al., ACS Nano 12 (2018) 7647–7662.
[95] X. Yu, D. Gao, L. Gao, J. Lai, C. Zhang, Y. Zhao, et al., ACS Nano 11 (2017) 10147–10158.
[96] J. Kim, W.A. Li, Y. Choi, S.A. Lewin, C.S. Verbeke, G. Dranoff, et al., Nat. Biotechnol. 33 (2015) 64–72.
[97] A.V. Kroll, R.H. Fang, Y. Jiang, J. Zhou, X. Wei, C.L. Yu, et al.,Adv. Mater 29 (2017), 1703969.
[98] Y. Dai, C. Xu, X. Sun, X. Chen, Chem. Soc. Rev. 46 (2017) 3830–3852.
[99] T. Ji, Y. Zhao, Y. Ding, G. Nie, Adv. Mater 25 (2013) 3508–3525.
[100] X. Zhang, C. Wang, J. Wang, Q. Hu, B. Langworthy, Y. Ye, et al.,Adv. Mater 30 (2018), 1707112.
[101] M.T. Chow, A.D. Luster, Cancer Immunol. Res. 2 (2014) 1125–1131.
[102] M.J. Smyth, E. Cretney, M.H. Kershaw, Y. Hayakawa, Immunol. Rev. 202 (2004) 275–293.
[103] A. Tanaka, S. Sakaguchi, Cell Res. 27 (2017) 109–118.
[104] A. La Cava, L. Van Kaer, S. Fu Dong, Trends Immunol. 27 (2006) 322–327.
[105] W. Ou, L. Jiang, R.K. Thapa, Z.C. Soe, K. Poudel, J.H. Chang, et al., Theranostics 8 (2018) 4574–4590.
[106] R. Noy, J.W. Pollard, Immunity 41 (2014) 49–61.
[107] G. Yang, L. Xu, Y. Chao, J. Xu, X. Sun, Y. Wu, et al., Nat. Commun. 8 (2017) 902.
[108] Q. Chen, C. Wang, X. Zhang, G. Chen, Q. Hu, H. Li, et al., Nat. Nanotechnol. 14 (2019) 89–97.
[109] Y. Qian, S. Qiao, Y. Dai, G. Xu, B. Dai, L. Lu, et al., ACS Nano 11 (2017) 9536–9549.
[110] P. Zhao, Y. Wang, X. Kang, A. Wu, W. Yin, Y. Tang, et al., Chem. Sci. 9 (2018) 2674–2689.
[111] Y. Yang, J. Tang, P.L. Abbaraju, M. Jambhrunkar, H. Song, M. Zhang, et al., Angew Chem. Int. Ed. 57 (2018) 11764–11769.
[112] Q. Liu, H. Zhu, K. Tiruthani, L. Shen, F. Chen, K. Gao, et al., ACS Nano 12 (2018) 1250–1261.
[113] Y. Fan, R. Kuai, Y. Xu, L.J. Ochyl, D.J. Irvine, J.J. Moon, Nano Lett. 17 (2017) 7387–7393.
[114] J. Lu, X. Liu, Y.P. Liao, F. Salazar, B. Sun, W. Jiang, et al., Nature Commun. 8 (2017) 1811.
[115] C. Wang, J. Wang, X. Zhang, S. Yu, D. Wen, Q. Hu, et al., Sci. Transl. Med. 10 (2018) 3682.
[116] Q. Liu, F. Chen, L. Hou, L. Shen, X. Zhang, D. Wang, et al., ACS Nano 12 (2018) 7812–7825.
[117] J.F. Lovell, T.W.B. Liu, C. Juan, Z. Gang, Chem. Rev. 110 (2010) 2839.
[118] D. Dolmans, D. Fukumura, R.K. Jain, Nat. Rev. Cancer 3 (2003) 375–380.
[119] D.K. Chatterjee, L.S. Fong, Y. Zhang, Adv. Drug Deliv. Rev. 60 (2008) 1627–1637.
[120] A.P. Castano, P. Mroz, M.R. Hamblin, Nat. Rev. Cancer 6 (2006) 535–545.
[121] L. Dai, K. Li, M. Li, X. Zhao, Z. Luo, L. Lu, et al.,Adv. Funct. Mater. 28 (2018), 1707249.
[122] C. He, X. Duan, N. Guo, C. Chan, C. Poon, R.R. Weichselbaum, et al., Nat. Commun. 7 (2016) 12499.
[123] W. Song, J. Kuang, C.X. Li, M. Zhang, D. Zheng, X. Zeng, et al., ACS Nano 12 (2018) 1978–1989.
[124] A.P. Castano, P. Mroz, M.X. Wu, M.R. Hamblin, Proc. Natl. Acad. Sci. U. S. A. 105 (2008) 5495–5500.
[125] D. Wang, T. Wang, J. Liu, H. Yu, S. Jiao, B. Feng, et al., Nano Lett. 16 (2016) 5503–5513.
[126] J. Peng, Y. Xiao, W. Li, Q. Yang, L. Tan, Y. Jia, et al.,Adv. Sci. (2018), 1700891.

[127] G. Liangran, D.D. Yan, Y. Dongfang, L. Yajuan, W. Xiaodong, Z. Olivia, et al., ACS Nano 8 (2014) 5670–5681.
[128] J. Nam, S. Son, L.J. Ochyl, R. Kuai, A. Schwendeman, J.J. Moon, Nat. Commun. 9 (2018) 1074.
[129] L. Zhang, D. Jing, L. Wang, Y. Sun, J.J. Li, B. Hill, et al., Nano Lett. 18 (2018) 7092–7103.
[130] Y. Min, K.C. Roche, S. Tian, M.J. Eblan, K.P. McKinnon, J.M. Caster, et al., Nat. Nanotechnol. 12 (2017) 877–882.
[131] M.B. Bernstein, S. Krishnan, J.W. Hodge, J.Y. Chang, Nat. Rev. Clin. Oncol. 13 (2016) 516–524.
[132] Y. Chao, L. Xu, C. Liang, L. Feng, J. Xu, Z. Dong, et al., Nat. Biomed. Eng. 2 (2018) 611–621.
[133] K. Lu, C. He, N. Guo, C. Chan, K. Ni, G. Lan, et al., Nat. Biomed. Eng. 2 (2018) 600–610.
[134] P.A. Baeuerle, C. Reinhardt, Cancer Res. 69 (2009) 4941–4944.
[135] H. Chen, W. Zhang, G. Zhu, J. Xie, X. Chen, Nat. Rev. Mater. 2 (2017).
[136] J.K. Willmann, N. van Bruggen, L.M. Dinkelborg, S.S. Gambhir, Nat. Rev. Drug Discov. 7 (2008) 591–607.

Dr. Weijing Yang received her PhD degree in Chemistry and Physics of Polymers from Soochow University (2017). She then joined Laboratory of Molecular Imaging and Nanomedicine (LOMIN), National Institutes of Health (NIH) supervised by Prof. Xiaoyuan (Shawn) Chen. Her current interests focus on polymer synthesis, drug delivery and exploiting nanotechnology for cancer immunotherapy.

Dr. Zijian Zhou received his PhD in Chemistry (Chemical Biology) from the Xiamen University in 2015. Then he joined the Laboratory of Molecular Imaging and Nanomedicine (LOMIN), National Institute of Biomedical Imaging and Bioengineering (NIBIB) at the National Institutes of Health (NIH), as a postdoctoral fellow. His research interest is cancer nanomedicine including novel imaging agents and strategies for cancer diagnosis, molecular imaging of cancer therapeutic response, and activatable systems for cancer theranostics.

Dr. Joseph Lau received his PhD from Faculty of Medicine, University of British Columbia in 2016. After two years postdoctoral training in University of British Columbia, he joined Laboratory of Molecular Imaging and Nanomedicine (LOMIN), National Institute of Biomedical Imaging and Bioengineering (NIBIB) at the National Institutes of Health (NIH) in 2018, as a postdoctoral fellow. His research interest lies in using nuclear theranostic agents for cancer immunotherapy.

Prof. Shuo Hu obtained her PhD from Xiangya Hospital, Central South University in 2004. She engaged at Tongji Medical College, Huazhong University of Science and Technology, as a postdoctoral fellow from 2008 to 2009. She acted as a visiting scholar in NIH from 2011 to 2012. Now she is doctoral supervisor and the chief of Department of PET Center, Xiangya Hospital, Central South University. Her interests lie in radionuclide imaging and therapy and she has abundant experience in clinical trials.

Prof. Xiaoyuan Chen received his PhD in Chemistry from the University of Idaho (1999). He started as an Assistant Professor in 2002 and then moved to Stanford in 2004. He moved to NIH in 2009 and became a Senior Investigator and the Chief of the Laboratory of Molecular Imaging and Nanomedicine (LOMIN) at the National Institute of Biomedical imaging and Bioengineering (NIBIB), NIH. His current research interests include development of a molecular imaging toolbox for a better understanding of biology, early diagnosis of disease, monitoring the therapy response, and guiding drug discovery/development. His lab puts special emphasis on high sensitivity nanosensors for biomarker detection and theranostic nanomedicine for imaging, gene and drug delivery, and monitoring of treatment.